AIRBUS

Review of Aeronautical Fatigue Investigations in Germany during the Period April 2015 to March 2017

Ottobrunn, 20th of April 2017

Elke Hombergsmeier
Airbus Group Innovations
Innovation Centre 1

TX1RP201720694 - Technical Report

Title
Review of Aeronautical Fatigue Investigations in Germany during the Period April 2015 to March 2017

Author
Elke Hombergsmeier

Phone	E-mail	Team/Work area
+49 89 607 20888	elke.hombergsmeier@airbus.com	TX1M

Contract or Proposal-No.	Project/ WP-N°	Roadmap Segment	Number of Pages	Date of Publication
-	-	-	52	April 2017

Customer name
-

Abstract:
This review represents a compilation of abstracts on aeronautical fatigue investigations in Germany during the period April 2015 to March 2017 and is presented within the scope of the Meeting of the International Committee on Aeronautical Fatigue in Nagoya, Japan, June 5th-9th 2017.

The contribution of summaries by German aerospace manufacturers, governmental and private research institutes, universities as well as aerospace authorities was completely voluntary, and is acknowledged with sincere appreciation by the author of this review.

Enquiries concerning the contents should be addressed directly to the author of the corresponding summary.

Keywords for database
International Committee on Aeronautical Fatigue, ICAF 2017, National Delegate Review

[1] Classification
1 Public Dissemination
2 Airbus Group Internal/Project Partner Use
3 Airbus Group Confidential
4 Airbus Group Secret

[2] National Government Classification
1 Yes
2 No

Acceptance

Elke Hombergsmeier	Ulrike C. Heckenberger	Elke Hombergsmeier
Author	**Head of Team**	**Roadmap Leader**

Table of contents

Tables

Figures

1 Introduction

This review represents a compilation of abstracts on aeronautical fatigue investigations in Germany during the period April 2015 to March 2017 and is presented within the scope of the Meeting of the International Committee on Aeronautical Fatigue in Nagoya, Japan, June 5th-9th 2017.

The contribution of summaries by German aerospace manufacturers, governmental and private research institutes, universities as well as aerospace authorities (Table 1) was completely voluntary, and is acknowledged with sincere appreciation by the author of this review.

Enquiries concerning the contents should be addressed directly to the author of the corresponding summary.

Table 1: Mailing addresses of contributing companies and institutes

Abbreviation	Details
ADS	Airbus Defence and Space, Airbus DS GmbH, Robert-Koch-Straße 1, D-82024 Munich, Germany, www.airbusdefenceandspace.com
AGI	Airbus Group Innovations, D-81663 Munich, Germany, www.airbusgroup.com
AIRBUS	Airbus Operations GmbH; Kreetslag 10, D-21129 Hamburg, Germany, www.airbus.com
DLR	German Aerospace Centre, Institute of Materials Research, 51147 Cologne Germany, www.dlr.de
GROB	Grob Aircraft AG, Lettenbachstrasse 9, D-86874 Tussenhausen-Mattsies, Germany www.grob-aircraft.com
HZG	Helmholtz-Zentrum Geesthacht; Max-Planck-Straße 1,D-21502 Geesthacht, Germany, www.hzg.de
IABG	Industrieanlagen-Betriebsgesellschaft mbH; PO-Box 1212, D-85503 Ottobrunn, Germany, www.iabg.de
IMA	IMA Materialforschung und Anwendungstechnik GmbH; Postfach 80 01 44, D-01101 Dresden, Germany, www.ima-dresden.de
ISD	Leibniz Universität Hannover, Institut für Statik und Dynamik (Institute of Structural Analysis), Appelstraße 9A, D-30167 Hannover, Germany, http://www.isd.uni-hannover.de
IVW	Institut für Verbundwerkstoffe GmbH, Erwin-Schrödinger-Str. 58, D-67663 Kaiserslautern, http://www.ivw.uni-kl.de
LMW	University of Siegen, Research Group for Material Science and Material Testing; Paul-Bonatz-Strasse 9-11, D-57076 Siegen, Germany, www.uni-siegen.de

2 Full Scale Testing

2.1 Airbus A350 XWB EF3 Fatigue Test

P. Boesch, S. Hilpert (AIRBUS)
Contact: peter.boesch@airbus.com

For the A350XWB aircraft full scale fatigue and damage tolerance testing of the structure was performed by Airbus (supported by suppliers) in three test cells by splitting the aircraft structure in a front, center (with wings) and rear test specimens. The focus of the three Fatigue test cell was on the metallic parts while the CFPR structure was validated mainly by demonstrators.

ONE Part of these full scale fatigue tests was the A350 XWB EF3 (Essai Fatigue 3) representing the aft and rear fuselage and lower VTP (Figure 1 and Figure 2). The test performance in the Airbus Test facilities in Hamburg was started in January 2014 with a static test phase followed in March 2014 by the main fatigue testing, which was completed in October 2015 having achieved 86.400 simulated flights equivalent to three design service goals (DSG).

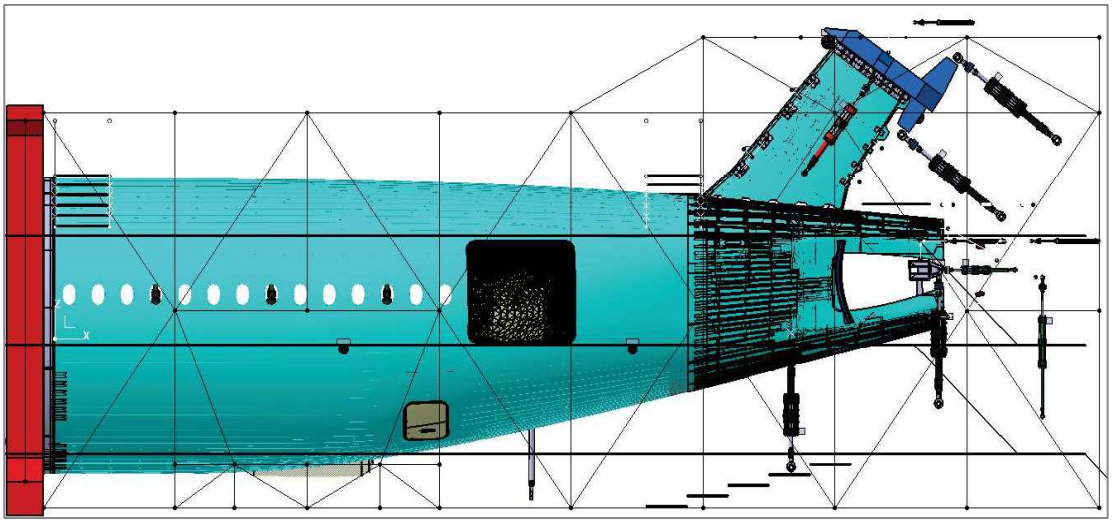

Figure 1: A350 XWB EF3 specimen and test set up (schematic view) at Airbus in Hamburg

During this period an intensive test program on a 24/7 basis was performed running nearly 15 million load cases and more than 86.400 pressurization cycles in less than 8.5 months of pure testing time. In addition to the pure testing time, planned inspection and regular measurement campaigns were performed. These tests stops were also used for test specimen modifications like the introduction of new artificial damages or the extension of existing ones.

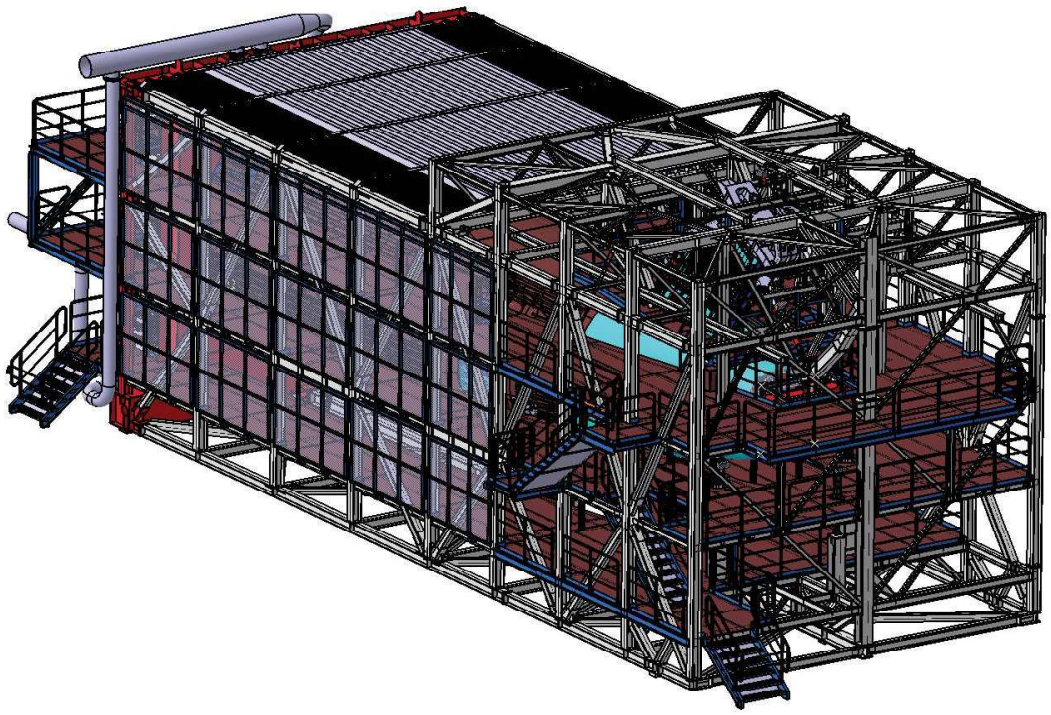

Figure 2: A350 XWB EF3 test set up at Airbus in Hamburg

The whole full scale fatigue test was equipped with roughly 1800 measurement channels and 28 loading actuators additional to the fuselage internal pressurization. Further special measurement techniques for static and dynamic measurements were applied: e.g. Structure Health Monitoring (SHM) systems for measurement of strain and impact detection, 3D optical measurement system and a Pre-Load Indication (PLI) system for determination of the preload (force) in the VTP tension bolts by ultrasonic pulse-echo method were used.

Between the end of 2015 and early 2016 the extended residual strength test program (RST) was performed to demonstrate the damage tolerance and robustness of the structure by applying maximum foreseen loads with additional artificial damage applied to the “aged” structure. Combining measurements, structure inspections and online monitoring of sensors during these tests provided relevant data for further analysis by AIRBUS stress departments.

The test has now been dismantled and tear down inspections have started on the test specimen structure for detailed analysis of the known damages and other critical areas of the structure at the end of its planned Fatigue life. The results will be used to improve reliability of the aircraft structure and to optimize the in-service inspection and maintenance tasks for the airlines.

2.2 Airbus A350 XWB Fatigue Testing – component tests at airbus structures test centre Hamburg

Rolf Hinrichs, Christian Göpel (Airbus Operations)
Contact: christian.goepel@airbus.com

In the frame of development and certification of the A350-900 XWB aircraft a huge amount of structural fatigue tests were performed spread over Europe. Content of this article is an overview of component tests performed at the Airbus Structures Test Centre in Hamburg from 2012 to 2016.

2.2.1 Root Joint Demonstrator (Figure 3)

This development test campaign was initiated for an early validation and verification of the design and sizing methods of the VTP root joint concept for A350XWB in order to minimize risk.
The purpose was:
• Validation of interface load distribution between S19 and VTP
• Validation of global and local FEM
• Identification of critical areas to metallic fatigue

Focus of this test project was the structural investigation of the interface with multi joint junction between rear end fuselage and VTP as well as global and local FEM validation with and without one fitting failed. In addition critical areas for metallic fatigue had to be identified and determined.

The test campaign was executed via the following main phases:
- First static phase: Static loading to validate FEM and load distribution.
- Fatigue phase: Fatigue loading to early identify the metal fatigue critical areas
- Second static Phase: Static loading at higher levels to evaluate non-linear effects due to gapping in the interface area with tension/shear bolts removed or not.

A prototype VTP stub box from root up to rib 5, without leading- and trailing edge, rudder and rudder hinge arms was manufactured. Above rib 4 the box was reinforced to connect the specimen with an upper load introduction device (upper box dummy).

All parts of the root joint between fuselage and the VTP and a full section 19 of the rear fuselage as Pre-Production Part were also subject for testing. For load introduction 14 hydraulic jacks were used to simulate representative root joint loading.

A truncated metal Fatigue flight-by-flight spectrum loading with 57,600 simulated flights (2 DSG) for “hot spot” detection with static reference load cases was applied in the fatigue phase.

All tests were performed in 2012.

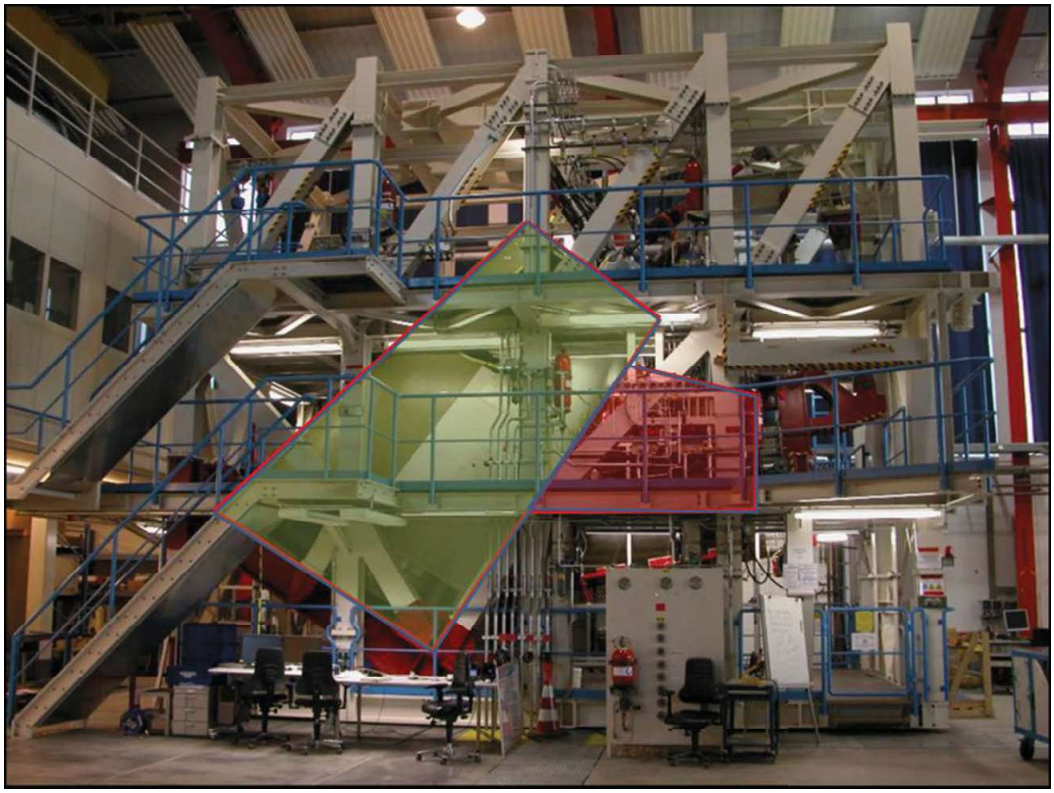

Figure 3: A350 Root Joint Demonstrator Test set-up

2.2.2 Full Scale test with the vertical stabilizer (Figure 4 and Figure 5)

The VTP Full scale Test was part of the A350 XWB aircraft certification tests. The test specimen comprised a serial VTP fin box including leading edge, trailing edge and rudder hinges. The VTP had been attached via the serial multi joint connection using tension and shear bolts with the rear fuselage Section 19 (S19) representative for load introduction purposes. Static and fatigue test phases were performed to provide:

- Validation of FE modelling and analysis.
- Limit load and ultimate load static strength justification
- CFRP damage tolerance and residual strength justification for CFRP VTP structure

Relevant loads coming from the rudder had been simulated by loading of each interface points between rudder hinges and VTP fin box. In order to avoid unintended misalignments of the hinge loading due to VTP deformation, the hinge brackets were coupled together along the hinge line with special supporting rods.

A total number of 20 hydraulic jacks were simulating the air loads on the VTP and the loads originating from the rudder interfaces. The loading in this test campaign shall be both, static and fatigue applying a flight by flight loading spectrum for the damage tolerance phase.

The fuselage S19 was only used as load introduction with representative rear fuselage stiffness and could be reused from the previously performed Root Joint Demonstrator Test.

Local damages from the former test campaign made a repair solution necessary before VTP-FST to incorporate a new set of metallic frames (FR94 – FR98) and new frame clips.

Tests were performed between April 2013 and August 2014.

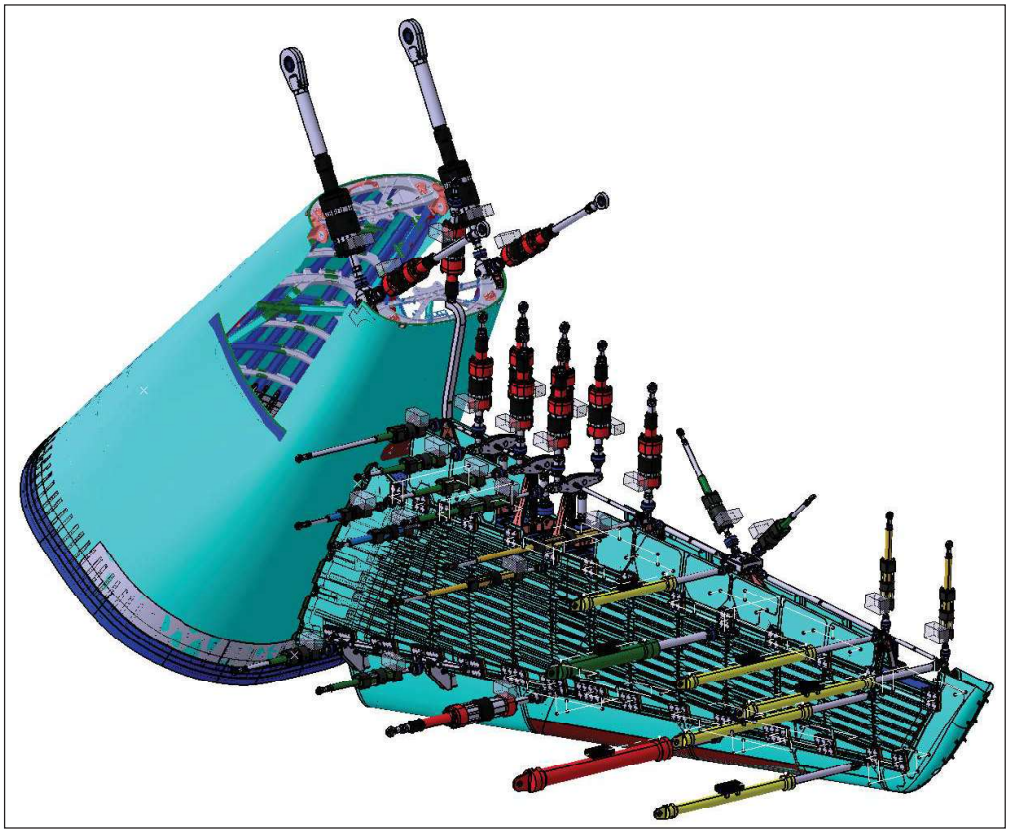

Figure 4: Loading concept for VTP full scale test with aft fuselage section 19

Figure 5: A350 VTP Full Scale Fatigue test set-up

2.2.3 Rudder full scale tests (Figure 6)

A test campaign with the A350 full scale rudder was performed to demonstrate structural integrity for the completely new developed rudder in composite CFRP design. For certification reasons two separated full scale tests for VTP and rudder were applied. A division between CFRP parts qualification and metal hinge and actuator fittings was decided using two separated tests with two rudder specimens from serial manufacturing.

The rudder consists mainly of two monolithic with stiffeners reinforced side panels coupled with a rudder spar and ribs without cut-outs.

The test rig was a closed steel frame-work construction with integrated platforms and stair cases for inspection purposes, wherein all applied test forces were internally supported. The specimen allocation in the test rig was selected to be horizontal with the hinge line downwards aligned parallel to the hangars floor. 29 servo-hydraulic jacks were used to apply distributed air loads on the rudder surfaces and to load the hinge line fittings with the reaction forces from the fin under most realistic conditions.

For both specimen static and fatigue test phases were planned.

2.2.3.1 Composite Fatigue Tests

The first specimen was foreseen for testing between 2013 and 2014 performing:

- Limit and ultimate static strength tests before first flight
- CFRP fatigue 1 DSG (28800 FC) with a specific CFRP load spectrum with omission.
- CFRP damage tolerance test ½ DSG followed by a residual strength test RST

2.2.3.2 Metal Fatigue Test

The Second specimen was operated between 2014 and 2016 for:

- Metal fatigue phase (1 DSG) using a metal fatigue load spectrum with truncation
- Damage tolerance phase (2 DSG) with fail safe concept for metallic fittings and introduced damage (e.g. saw cuts, missing fasteners)
- Repair and margin research test

Figure 6: A350 Full scale rudder test set-up

2.2.4 Outer Flap Metal Fatigue Test A350-900 (Figure 7)

A campaign with an A350-900 outer flap including supports 3 & 4 was performed in Airbus Hamburg Test Centre between 2014 and 2016. Aim of this test procedure was the verification and validation of the fatigue and damage tolerance behaviour of the metal parts of the A350-900 Outer Flap and Support Structure in order to support the certification of the A350-900 High Lift structures. A fatigue life of 3 DSG (1 DSG =28800 flights) was applied by a flight-by-flight fatigue test spectrum. For specimen a right hand outer flap with supports 3 and 4, with various artificial damages in the metal parts as well as in the CFRP structure was used.

In addition, the support structure's kinematic was tested. The motion concept was reversed compared to the original aircraft concept. Therefore a wing dummy structure, which holds the supports, was rotated around the hinge line for flap settings from -2° to 37.5° while the flap itself was kept in its position. The specimen was exposed to air loads as well as loads coming from the fairings, support 5 and wing. In total 28 servo-hydraulic loading jacks applied these loads. A special test rig was designed and manufactured for this test, enabling the kinematics' movements by electric screw drive mechanism and distributed load introductions on the flap skin surface.

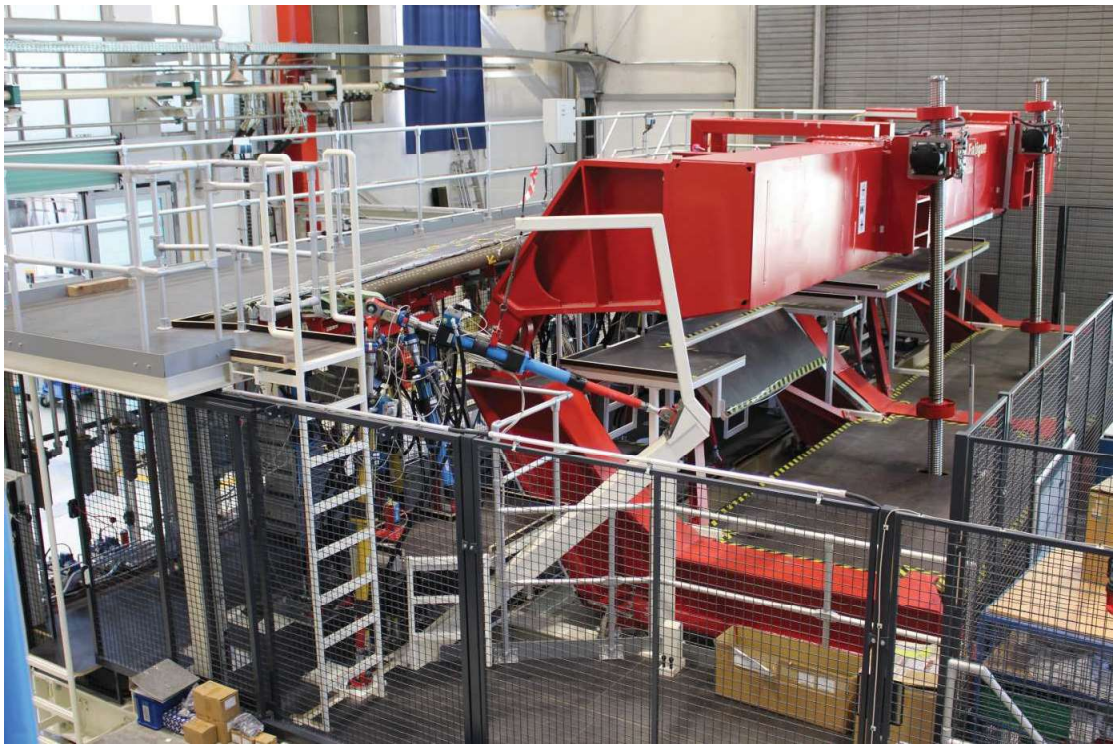

Figure 7: A350-900 Outer Flap Fatigue Test set-up

2.3 Airbus A350 XWB EF2 Fatigue Test

O. Tusch (IABG)
Contact: hilfer@iabg.de

In early 2014 the full scale fatigue test A350 XWB EF2 (Essai Fatigue 2) (see Figure 8) representing the fuselage centre section and both wings was started and in early autumn 2016 already three design service goals equivalent to 86.400 simulated flights were reached.

Figure 8: A350 XWB EF2 test set up at IABG

During this period an intensive test program on a 24/7 basis was performed running over 15 million load cases and more than 86.400 pressurization cycles in less than roughly three quarters of a year of pure testing time. In addition to the pure testing time, planned inspection and modification stops with over 7.000 hours of inspection were performed and regular structural health monitoring measurement campaigns were recorded.

The whole full scale fatigue test is equipped with roughly 4.000 measurement channels which are continuously loop recording the 100 Hz data stream in order to allow full analysis of any findings on the progress of artificial damages during the test.

Between the end of 2016 and early 2017 the extended residual strength test programme (RST) is performed to demonstrate the damage tolerance and robustness of the structure by applying maximum foreseen loads with artificial damage applied to the structure (Figure 9). Combining measurements, flexible in-depth inspections and online monitoring provides sophisticated data for further analysis by AIRBUS.

Component stress teams are monitoring the RST campaign closely by means of live data acquisition stations showing readings and predictions of hundreds of strain and load channels during the different RST load cases representing loading up to limit load.

Figure 9: A350 XWB EF2 RST Campaign up bend case

A detailed presentation of the virtual test setup simulation which has been performed to prepare and run such a sophisticated test fulfilling the customer test speed and accuracy expectations is given in the presentation “Fatigue testing of new generation wide body aircraft at benchmark level” presented during the ICAF Symposium 2017.

2.4 BD500-DADTT - Durability and Damage Tolerance Test

Thomas Jung (IABG)
Contact: hilfer@iabg.de

The DURABILITY AND DAMAGE TOLERANCE TEST (DADTT) for the type certification of Bombardiers CSeries (BD500) CS100 / CS300 aircraft family started on schedule in August 2014 at IABG in Dresden. The testing is carried out on the CS100 model and will also obtain sufficient data to enable successful certification of the CS300 aircraft. The Durability, Damage Tolerance and Residual Strength of the aircraft metallic structure will be covered by the DADTT.

The BD500 metallic structure must be subjected to a Durability and Damage Tolerance test program to show compliance with:

1. Transport Canada certification requirements for transport category airplanes.
2. FAA and EASA certification requirements for large airplanes.

The metallic structure of the airframe shall be subjected to spectrum loading for a minimum of 3 times the Design Service Goal (DSG), i.e. 180,000 flight cycles, followed by a residual strength test and a teardown inspection.

BD500-DADTT test phases:

1. PREPARATION PHASE
    a. Initial Inspection
    b. Leakage test
    c. Commissioning
2. PHASE 1 – DURABILITY TESTING
    a. Testing to 2 DSG of flight cycles (120,000 total flights) without artificial damages
3. PHASE 2 – DAMAGE TOLERANCE TESTING
    a. Testing to 1 DSG of flight cycles (additional 60,000 flights) after introduction of artificial damage – analyse crack propagation and demonstrate endurance
4. PHASE 3 – RESIDUAL STRENGTH TESTING
    a. Demonstrate the structural integrity of standard repairs
    b. Validate the critical crack lengths of the PSE analysis
    c. Artificial damages to be extended and additional ones to be introduced
5. PHASE 4 – TEARDOWN INSPECTION

The test specimen consists of:

1. The pressurized fuselage extending from frame C277 to C1476
2. The right and left outer wing boxes attached to the centre wing box
3. Vertical stabilizer incl. rudder
4. Main and nose landing gear (partly)
5. Dummy structures
    a. Horizontal stabilizer
    b. Main and nose landing gear
    c. Engine pylons
    d. Flaps, ailerons, slats
    e. Winglets

Typical repairs for metallic structure will be introduced at the beginning of the first DSG in order to validate the Structural Repair Manual.

Artificial damage has been introduced into the structure at the beginning of the third DSG, after 120,000 flight cycles have been achieved.

In total the BD500 specimen is loaded by 124 hydraulic jacks and 7 restraints. Measurement of strains and deflections with up to 1500 Strain Gauges and Displacement Transducers is required (Figure 10).

Figure 10: Overview of the BD500 Fatigue Test Set-up at IABG

2.5 G120TP Wing Static & Fatigue Test for MTOW Increase

Bernd Zapf (GROB)
Contact: B.Zapf@grob-aircraft.com

The GROB Aircraft AG will increase the Maximum Take-off Weight (MTOW) for the model G120TP-A. For this Major Change program GROB Aircraft will perform a Wing Static & Fatigue Test (Figure 11).

The purpose of the test was to verify that the wing structure and its interfaces to the fuselage are able to support limit load without detrimental, permanent deformation and can sustain ultimate load for at least three seconds for the increased loads relating to an increased MTOW of the G120TP. Aim of the failure load test was to determine the rupture load and the failure mode of the wing structure. During the specified tests wing up-bending loads were applied at a temperature of 72°C. Strains and deformations under load were measured in order to allow comparison with the results of previous strength tests, e.g. the WST and WFT of the G115TA performed by GROB Aircraft.

The test set-up was built up in the test hall at IABG Ottobrunn (Figure 12). An arrangement with the test article installed upside down was chosen in order to minimize the efforts related to the loading rigs. Therefore, the two hydraulic actuators (1 per semi-span) could be mounted to the rails of the test hangar's strong floor using existing T-slotted plates and bearing brackets. These actuators were connected to customized whiffle trees which distributed their load to five contour boards per semi-span. The test article itself was fixed to the test rig using the auxiliary provisions at the firewall frame and at the centre fuselage as interface. Furthermore, an adequate control and monitoring system (CMS), a data acquisition system (DAS) and a thermal chamber with controlled heater blowers were used for the tests. The rig was designed and sized for application of a wing up-bending load of 72 kN (maximum actuator load; equivalent to approx. 240% LL) per semi span using CAD models of the test article in unloaded condition.

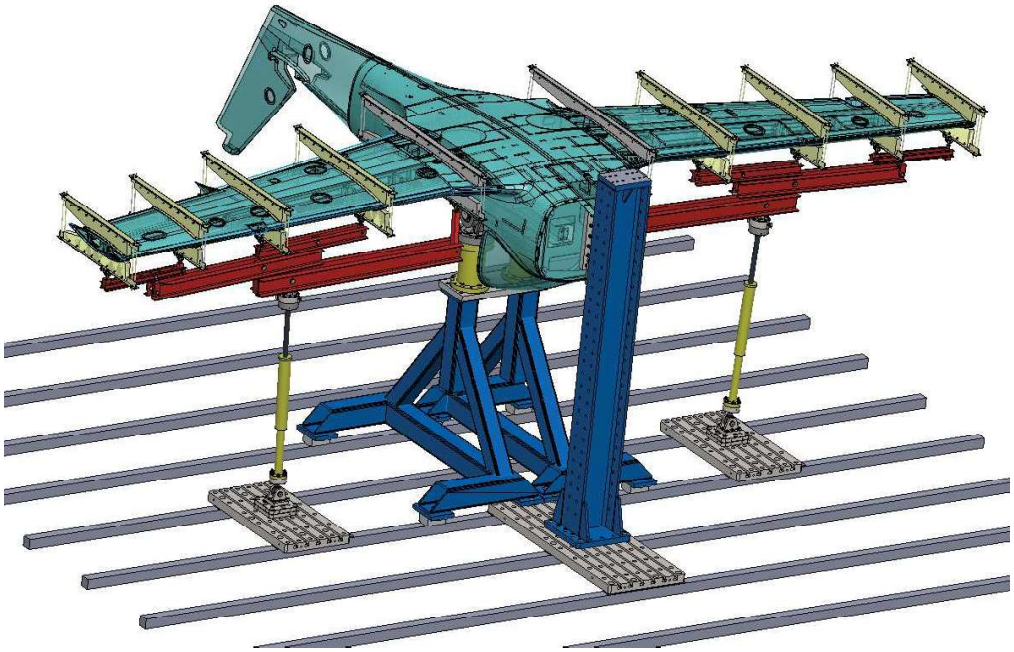

Figure 11: CAD Model of the test set-up

Figure 12: Test Set-up including thermal chamber at IABG

3 Fatigue and Fracture of Fuselage Panels and Joints

3.1 Curved panel fatigue and damage tolerance testing

Mirko Sachse, Silvio Nebel (IMA)
Contact: Silvio.nebel@ima-dresden.de

For Airbus research projects IMA Materialforschung und Anwendungstechnik GmbH (IMA Dresden) performed fatigue and damage tolerance tests of several curved fuselage panels. The test conditions covered internal pressure loads with superimposed axial tension loads. All panels were loaded with complex flight-by-flight load spectra. Targets for the different panels were:

- Investigate design life of current and future fuselage designs
- Investigate crack growth and repair methods under fatigue loading

The panels under investigation had different design approaches:

1. “Classic” design with longitudinal and circumferential joints (Figure 13)
2. Friction stir welding longitudinal joints and welded stringers
3. Fiber metal laminate skin

One panel was subjected to fatigue testing only. For the damage tolerance test the panel contained artificial damages to determine crack growth properties. With multiple panels the characteristics for different kinds of damages were investigated. This included, e.g. saw cuts in various areas of interest or longitudinal cracks across broken frames. The test program was accompanied by static tests. In particular, after reaching an extension of a 2-bay crack, the residual strength properties under over-pressure conditions were determined.

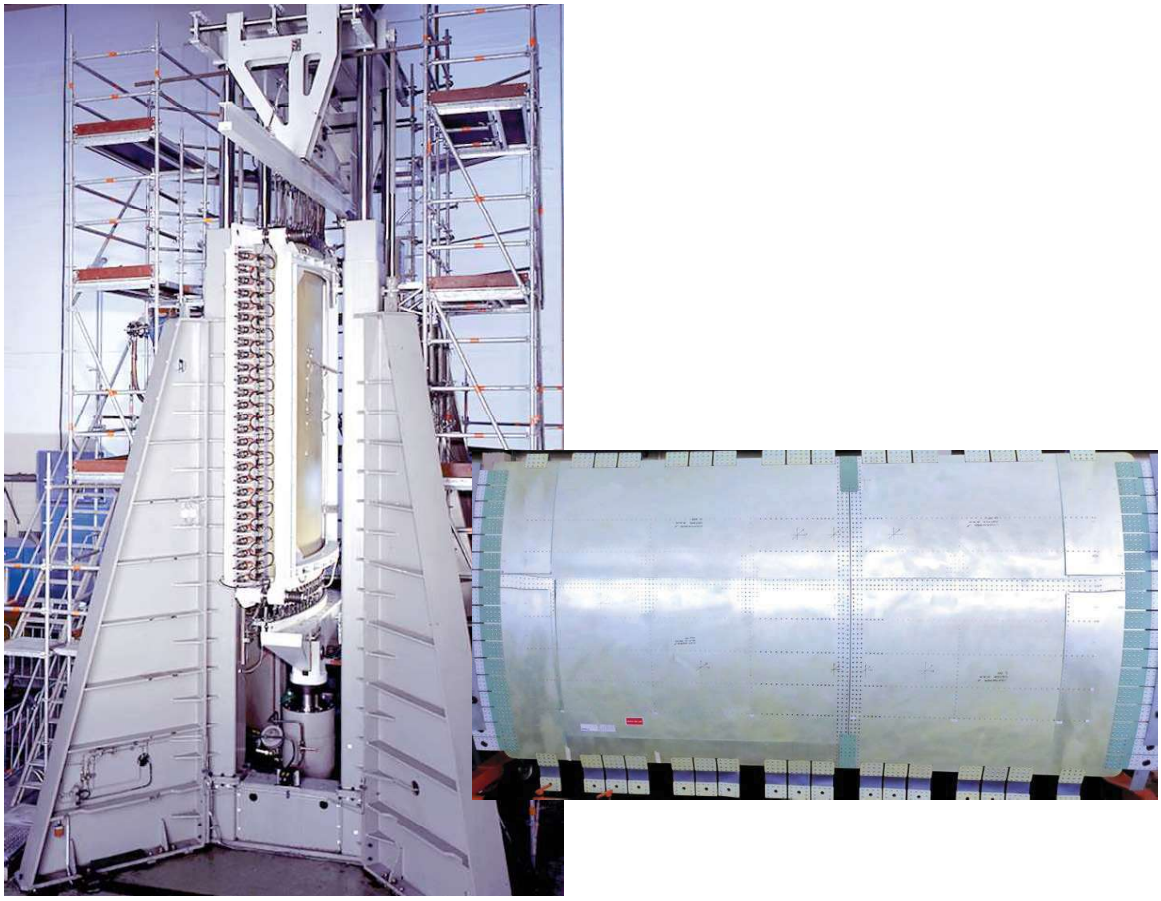

Figure 13: Panel with Longitudinal and Circumferential Joint

3.2 Curved Fuselage Panel with Door and Window Structures

Mathias Götze, Mirko Sachse, Silvio Nebel, Martin Semsch (IMA)
Contact: Silvio.nebel@ima-dresden.de

Within the European research project MAAXIMUS, IMA Materialforschung und Anwendungstechnik GmbH (IMA Dresden) performed tests on a CFRP fuselage panel including door and window structures (Figure 14). The panel size was 5.7 x 4 meters. The test conditions covered superimposed combinations of mechanical loads (axial tension and compression, bending, torsion, shear) and internal pressure. In addition, floor loads were considered using specific servo-hydraulic loading systems.

The main focus of the tests was to ensure representative loading conditions within the panel for parts of the fuselage, which are characterized by highly complex loading conditions. During the tests deformations and strains were measured using approximately 800 strain gauges and digital image correlation systems. To proof structural integrity the

influence of manufacturing flaws and artificial damages (BVIDs, VIDs and saw cuts) was investigated.

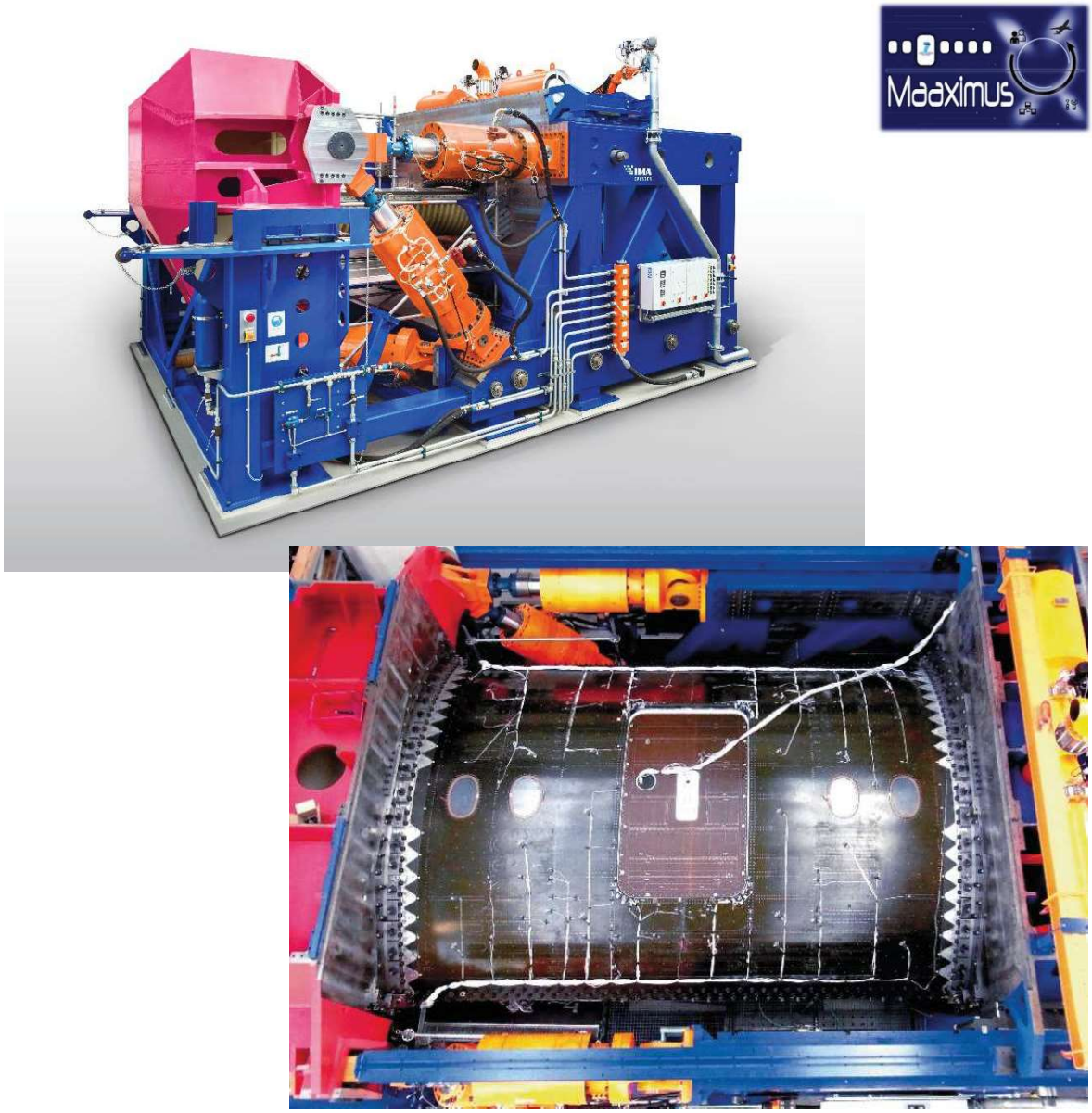

Figure 14: Test Set-up and Panel Structure

3.3 G120TP Component Fatigue Test Root Rib with Glass Roving

Bernd Zapf (GROB)
Contact: B.Zapf@grob-aircraft.com

This component fatigue test is part of the qualification procedure for the alternate E-glass roving type EC9 756 P109. The fatigue verification of the alternative material EC9 756 P109 are done with a component test on the root rib of the G 120TP-A wing (Figure 15). The glass roving is used in the root rib at the support structure for the shear bolts. This location is a highly loaded structural item due to the introduction of the wing shear forces. Therefore the root rib is representative in order to show the capability for the required interlaminar shear strength. Demonstration of the fatigue strength of the G 120TP-A wing is based on a full-scale fatigue test. The component fatigue test of the root rib with the glass roving EC9 756 P109 is performed by comparison with the standard roving in use.

A simplified, damage equivalent spectrum will be used, followed by a residual strength test at 72° C similar to the certification test.

The spectrum used for the fatigue test is a modified KoSMOS spectrum, including additional 800 limit load cycles to account for the aerobatic manoeuvers. By simulating 30 000 flight hours (load enhancement factor of 1.13), a fatigue life of 15 000 flight hours has been demonstrated in the certification fatigue test. For the fatigue test of the root rib, the modified KoSMOS fatigue spectrum are replaced by a condensed spectrum for constant amplitude testing, which shows damage equivalence. To develop damage equivalence the modified KoSMOS spectrum are replaced by an equivalent stepped spectrum; Using the stepped spectrum and the S-N curve of bonded joints. An accumulated damage is calculated based on the approach of Liu/Zenner. In this approach, the basic theory of a linear damage accumulation according to Palmgren/Miner is used. A damage equivalent block of 3 680 cycles with enhanced limit load amplitude (27 074 N x 1.13 to -6 953 N x 1.13) per 6000 FH has been determined, and therefore a damage equivalent block of 18 400 cycles per 30 000 FH.

The test rib is mounted on a steel plate using the forward and mid shear bolt. Additionally, the rib web are fixed to the steel plate by 15 bolts in order to represent the stiffness and support effect of the main spar, which is not part of the test. The upper and lower flanges are additionally supported by fittings as they are in the wing structure. The mid shear bolt of the test rib is supported in a ball bearing. The lever for load introduction needs to be 21.5 mm to reproduce the installation conditions in the A/C.

Figure 15: Test Set-up at the Test-Center “REALTEST GmbH”

3.4 The hybridized application of crenellation and laser heating techniques in improving the fatigue performance of airframe structures

J. Lu, N. Huber and N. Kashaev (HZG)
Contact: nikolai.kashaev@hzg.de

Fatigue is a primary concern in the design of airframe structures. Numerous researchers have proposed various local engineering techniques, such as crenellation [1] (Figure 16(a)-(b)) and laser heating [2,3] (Figure 16(c)-(e)), to further improve the fatigue performance of the airframe structures. Previously those techniques were only investigated separately. However, in real applications it is possible to apply them in a combined way, which can exploit the collaborative effects between different techniques and achieve a much more pronounced fatigue life extension.

This study is aimed at finding out the optimized configuration when hybridizing the crenellation and laser heating techniques, in which the fatigue crack retardation is achieved by systematic modulation of panel thickness and by superposition of a beneficial residual stress field. To achieve this goal, an advanced FEM-genetic algorithm coupled approach is proposed [4], where each possible configuration in terms of crenellation geometry and positioning of heating lines is encoded in a set of a binary string. FEM models corresponding to each configuration are automatically generated and the fatigue performance is predicted. The binary strings that represent the best configurations are then selected and recombined to form new strings potentially leading to better designs.

The inclusion of the residual stress field of laser heating in the FEM model is achieved by mapping the inherent strain distribution around the heating line. Its magnitude is attenuated with increasing thickness of the heated region. The interaction between inherent strain and local thickness is taken into account by a damping coefficient M, which increases stepwise in four scenarios of optimizations covering cases from no interaction up to strong interaction.

As shown in Figure 17(a), for the three cases of M = 0, 0.4, and 1 both heating lines are ideally placed at the center of the bay, whereas for the case of M = 2 the heating lines are placed more close to the stringers (at the border between section II and III). The crenellation designs evolved can also be classified into the same two groups. For the cases of M = 0, 0.4 and 1, the optimum crenellation patterns are very similar. The major difference among these solutions is that for M = 0 and 0.4 the thickness of section V is at the upper boundary of the thickness range (4.15 mm), whereas for M = 1 it is significantly reduced. For the case of M = 2 the crenellation pattern has a more distinct appearance. It is characterized by a wide region between the stringers and the heating lines, where the thickness stays at the lower boundary (1.9 mm).

In all the four scenarios it was found that the optimized configuration shows a significant fatigue life extension, which is larger than the linear superimposition of the fatigue life improvements achieved by each individual technique (Fig. 2(b)).

The amplification by combining both techniques was found to be the most pronounced when the damping coefficient is below 0.4. The optimized designs of this study can provide theoretical guidance for future experimental studies on the hybridized application of crenellation and laser heating techniques.

The proposed approach can also be applied to other design optimizations of fatigue resistant structures, which involve multiple fatigue crack retardation techniques.

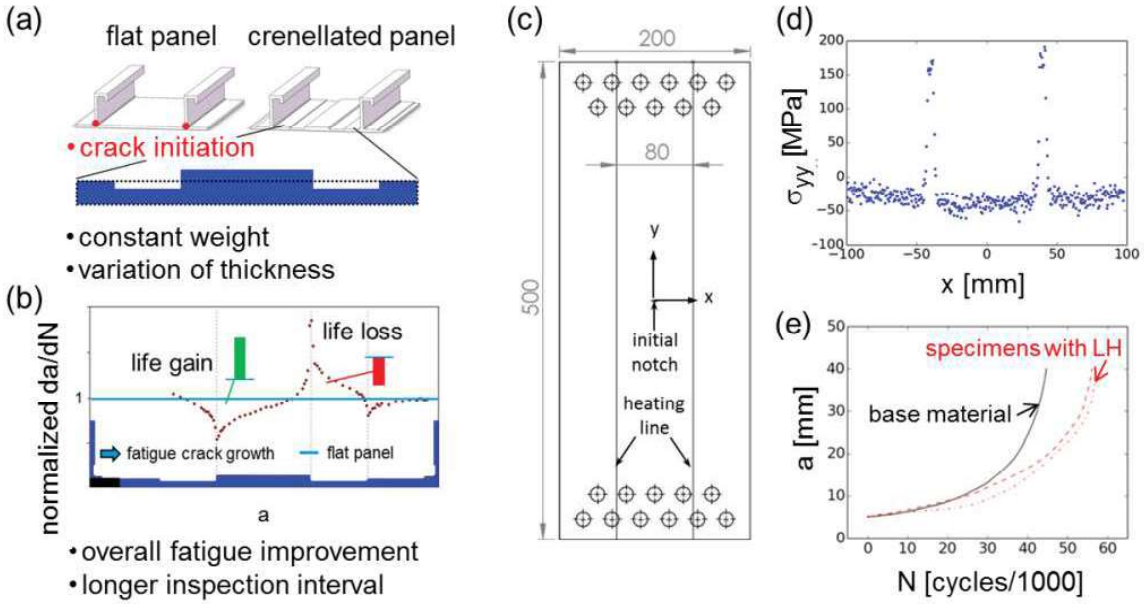

Figure 16: (a) Flat and crenellated panel with the same weight, (b) *da/dN* - *a* profile in crenellated stiffened panel normalized to that in a reference (flat) panel (blue line) with the same weight after [1]). Experimental data of laser heated AA2024 panels [3]. (c) Specimen geometry, (d) residual stress distribution in specimen with two laser heating lines measured using synchrotron X-ray diffraction and (e) comparison of fatigue performance between the base material and the laser heated specimens.

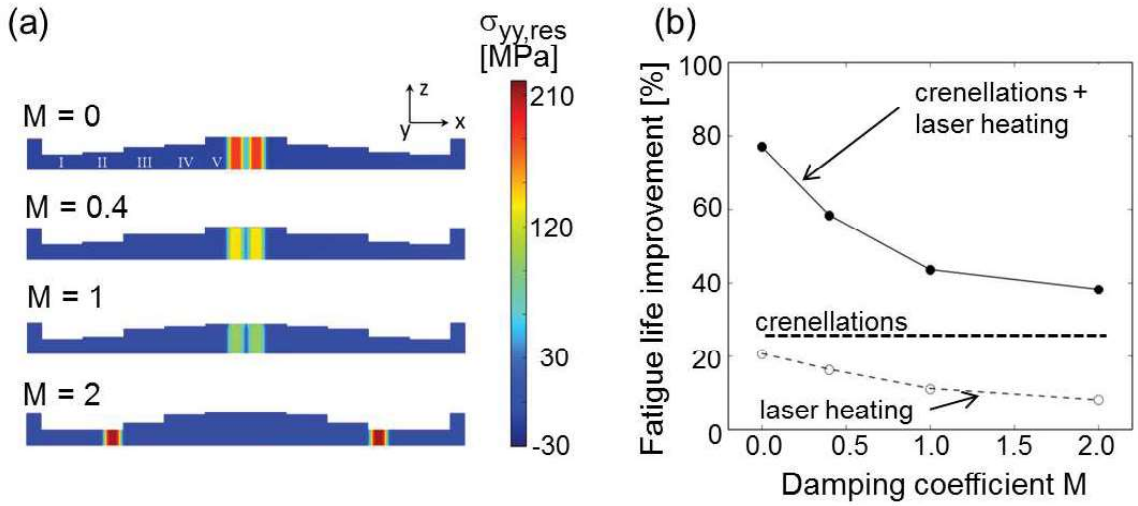

Figure 17: (a) Optimized crenellation geometries together with the optimized positions of laser heating lines, indicated by the superimposed color map showing the residual stress distribution for different damping coefficients, *M*. (b) Fatigue life improvement achieved by the optimized combinations of the crenellation and laser heating techniques for various damping coefficients in comparison with the maximum fatigue life improvement achieved by each individual technique.

References

[1] M.-V. Uz et al. (2009), *Int. J. Fatigue,* 31, pp. 916-926.
[2] D. Schnubel et al. (2012), *Mater. Sci. Eng. A*, A546, pp. 8-14.
[3] A. Groth et al.(2014), In: Proc. of the 29th Congress of the International Council of the Aeronautical Sciences, St. Petersburg, Russia.
[4] J. Lu et. al. (2016), *Eng. Fail. Anal*., 63, pp. 21-30.

4 Fatigue Life Assessment and Prediction

4.1 Prolonging Usage of the Tornado Fleet – Methods and approach of the German Air Force Service Life Enhancement

Daniel Raatz (ADS)
Contact: daniel.raatz@airbus.com

With novel defence scenarios the usage profiles of many aircraft in service have changed within the recent years and decades. This also often led to the necessity of maintaining them longer operable as initially intended, may it because they are suitable for novel scenarios, no later aircraft available can cover or because of resource considerations making the service prolongation of already existing aircraft more attractive than the development of new platforms. In case of the German Tornado fleet, both aspects let to the decision of extending its service life. The aircrafts outstanding reconnaissance, low-level and air to ground performance are a crucial part of the German Air Forces tactical capabilities. Additionally, extensive in-service experience, continuous system development and amortization have led to operational efficiency.

Apart from systems and equipment which are qualified differently, the currently qualified usage period for Tornado airframes can be expressed in a certain amount of Performance Design Requirement Flight Hours (PDR FH). They are based on a specific usage spectrum, comprising single missions with their manoeuvres which have been defined during the development of Tornado. In order to verify its analytical implementation, the therefrom derived spectrum has been tested on Tornados structure by Major Airframe Fatigue Test (MAFT). The thereby gained fatigue life qualification until end of testing is n PDR FH. Whereas the relation between PDR FH and Test Hours (TH) is: PDR FH = TH/SF, with SF being a Scatter Factor of SF>1, covering uncertainties in testing. It is within the responsibility of individual national operators to translate the fatigue qualification in PDR FH into a usable Flight Hour based service period. For the German Tornado fleet, this is performed by IABG GmbH, operating the LEDA- monitoring system. As the thereby monitored qualification will be reached in foreseeable future, a new service requirement has been defined by its operator. It was determined to be x FH, to be usable by the German Air Force. The gap between current qualification in PDR FH and future requirement of x FH has to be closed by a service life prolongation project which was named Service Life Enhancement (SLE) and aims at extending the Tornados airframe usage as follows:
One of the SLEs basic principles is to use a larger portion of its test-derived fatigue life qualification. For the current service period, a certain fraction (k) of the 0 to n TH has been used, hence:

$$k < n.$$

This is due to the fact that structural fatigue defects, detected during testing have to be covered by inspections and repair measures on the test itself and hence on in-service aircraft in order to use a respective test period as service life qualification. Since definition, development and implementation of such actions represent a major effort and constraints in aircraft operation; only a part of the test qualification was transformed into an

in-service qualification which was seen as being sufficient at that time. Consequently, it is now one subject of the SLE to translate further MAFT test evidence into usable service life by determining specific test damage induced actions and their point of implementation with respect to individual aircraft life consumption.

The second aspect that is made use of is the severity of in-service usage versus the design spectrum in terms of manoeuvres, actually flown. For instance, the frequency of in-service g-accelerations with certain magnitudes turned out to be less than defined in the design spectrum. Effects like this led to generally lower fatigue life consumption than initially dimensioned. One in service FH, causing a damage of $D_{I\text{-}S\ FH}$ consumed generally less life than one design PDR FH with its Damage $D_{PDR\ FH}$, hence:
$D_{I\text{-}S\ FH} < D_{PDR\ FH}$

The utilization of this effect demands for aircraft-individual in-service loads monitoring as the severity of single manoeuvres has to be set in relation to the designed manoeuvres and their occurrence.

Realization of the SLE approach is carried out by following steps. The major aspect in life prolongation is coverage of potential and existing damage and defects. As Tornado is designed and qualified by the safe-life philosophy, its airframe has to be by definition crack-free throughout the entire operation. Exceptions are to be qualified separately. In order to cover all expected damages, affected parts from testing- and in-service defects were registered. Further completion was gained by incorporating the results of a former major project in which structural critical items were defined by various other criteria. The entity of those parts was integrated into the so called Structural Qualification Register (SQR), which is a database, comprising all parts to be considered during SLE. Amongst other information, individual fatigue life qualification for each part is implemented in the SQR. This qualification is based on test- or in-service evidence; depending on the parts build standard and additional damage aspects like wear and tear or corrosion. Further, the parts PDR FH requirement until the aimed Out of Service Date (OSD) as well as their accumulated fatigue life consumption is listed. This requires a detailed analysis of the LEDA - life monitoring, relating each single part to specific monitoring parameters. In order to perform this and for establishing a certain order within the plurality of parts to be considered, they have been associated with their major loading actions and further grouped into specific load paths which can be covered by individual monitoring locations of LEDA. As a result of this, the fatigue life requirement from the current state until x FH can be compared against its qualification left on individual parts level. The life requirement is either met in case the remaining qualification is higher than the predicted life consumption until OSD or not. In case the requirement is not met, respective actions have to be performed in order to prolong the affected structures fatigue life. These actions consist of the entire life-enhancement measure spectrum available such as repair solutions, replacement of affected parts, local structural modifications by redesign or reinforcement and inspections. The choice of method is thereby dominated by aspects like the parts failure criticality, accessibility, observed mode of failure, implementation effort and so forth.

The German Air Force has already reduced its Tornado fleet by a significant number, putting pressure regarding fleet availability on each individual aircraft. This is the reason why measures to reach the desired OSD have to be in line with the fleet's maintenance schedule, avoiding additional service interruptions as they had been accepted in the UK MLFP which was the British Tornado life prolongation. Here, all measures were performed in one singe time consuming campaign. The alignment of SLE-actions with the regular maintenance schedule calls for an understanding of all potentially necessary measures that may arise until OSD. This picture must be as complete as possible in order to avoid missing one time opportunities for implementations only possible at non-recurring performed actions like fuselage segment separation.

The nature of the herein described approach (Figure 18) is that all affected parts and actions have to be known in advance or at least in due time while approaching the OSD. This means, that individual measures have to be known and prepared before their latest possible point of implementation which often is a matter of considerable time periods as long term processes like spare part manufacturing have to be initiated ahead.

It is the intention of the hereby proposed contribution to explain the overall approach of SLE with focusing on major aspects like Structural Health Monitoring, Fatigue testing evaluation, aging fleet management, risk mitigation and the context in which those aspects relate to each other.

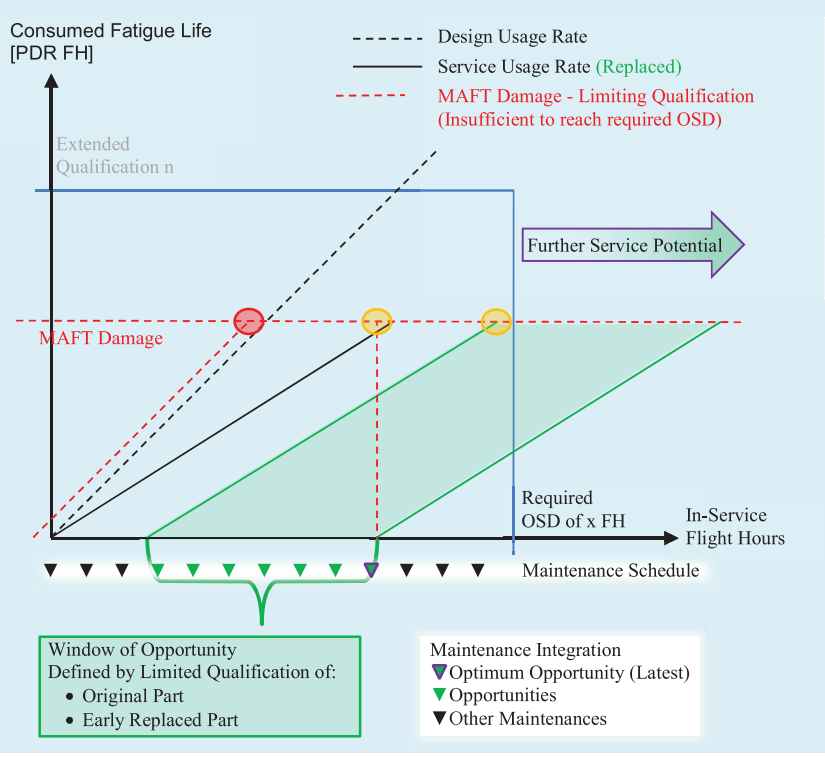

Figure 18: Window of Opportunity and Optimised Implementation of Parts Replacement with Respect to Further Service Potential and Utilization of Original Parts Qualification.

5 Fatigue and Fracture of Metallic Fuselage Materials

5.1 Crack Growth Behavior of Aluminum Wrought Alloys in the Very High Cycle Fatigue Regime

F. Bülbül, T. Stein, T. Kirsten, A. Brückner-Foit (IfW), M. Zimmermann (ifWW), H.-J. Christ (LMW)
Contact: fatih.buelbuel@uni-siegen.de

Due to their low density, excellent weldability, good mechanical properties, and favorable material costs the aluminum wrought alloys EN-AW 6082 and EN-AW 5083 are suitable for aeronautical components. In the regime of Very High Cycle Fatigue (VHCF), crack initiation was often found in the interior underneath the material surface [1, 2]. The VHCF crack growth behavior in particular of long cracks is not understood in detail. Therefore, it is necessary to perform fatigue experiments in air (representing fatigue crack growth from surface cracks) and in vacuum (representing fatigue crack growth in the interior of the component) in order to separate environmental effects on the fatigue crack propagation.

For this purpose an ultrasonic fatigue testing system (USFT) equipped with a small vacuum chamber was applied and tests were performed at constant stress amplitude. Semi-automatic controlled ΔK experiments were realized by applying a miniature fatigue testing system. This system was specifically designed for the use in a scanning electron microscope (SEM) and enables the in-situ observation as well as characterization of the crack growth behavior at high resolution under the vacuum conditions of the SEM and ex-situ in air without dismounting the specimen from the loading stage during examination. A micro-notch was prepared prior to the fatigue tests and the load ratio was R = -1.

The results obtained by the USFT show that the VHCF long crack growth in vacuum is very slow and differs in terms of the crack growth behavior from the Low Cycle or High Cycle Fatigue regime. Despite of long crack length, there are sections where stage I crack growth takes place. Crack propagation on single slip (marked with red arrows) and multiple slip systems were (blue arrow) detected (Figure 19a). At these sites it could be confirmed that the VHCF long cracks in vacuum behave similarly to microstructural short cracks. Therefore, microstructural features such as grain boundaries can decelerate the crack propagation, where the grain orientation of the adjacent grain plays a crucial role. By means of the miniature fatigue testing system in the SEM, it was determined that the impeding effect of grain boundaries as barriers is very high, if the Schmid factor in the adjacent grain is very low and vice versa. As it can be seen in Figure 19b, the primary crack was arrested at a grain boundary (black marked cycle). Despite of increasing ΔK no crack propagation in this area was detected, rather an additional crack was formed which propagated in grains with high shear stresses. Compared to vacuum, crack propagation in air was detected at reduced stress intensity factors how it can be seen in Figure 19c. In air, clusters of primary Mg_2Si-precipitates act as further barriers near the long crack propagation threshold value.

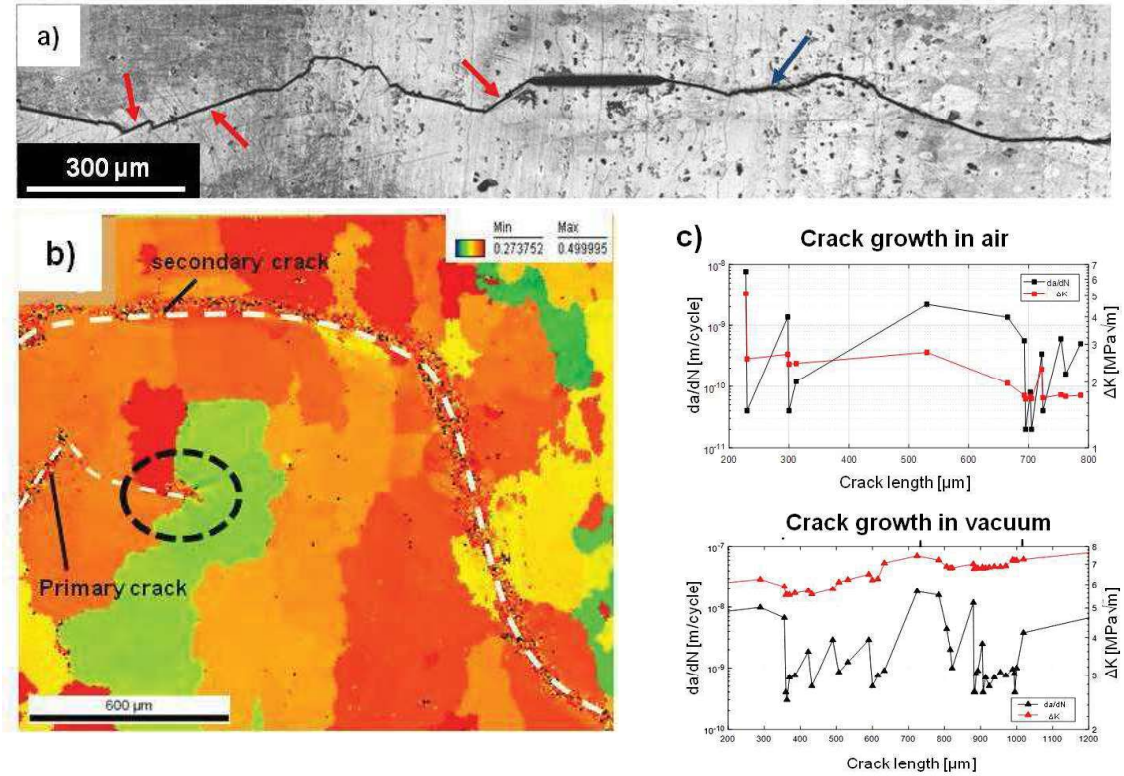

Figure 19: a) VHCF long crack path in vacuum showing crack growth in single slip (red arrows) and multiple slip (blue arrow), b) primary crack blocked at a grain boundary due to low shear stress in the adjacent grain and c) curves showing the stress intensity factors and the corresponding crack propagation rates in air and in vacuum

Against this background, a two dimensional numerical short fatigue crack growth model was adapted leading to a realistic simulation of the long fatigue crack propagation in the VHCF regime. The model can be applied to synthetic microstructures allowing a physically based assessment of the effect and relevance of microstructural parameters on the VHCF life, which is determined by microstructure-controlled long fatigue crack growth.

Acknowledgement
This work is funded by Deutsche Forschungsgemeinschaft (DFG).

References

[1] H. W. Höppel, M. Prell, L. May, M. Göken: Influence of grain size and precipitates on the fatigue lives and deformation mechanisms in the VHCF-regime. Procedia Engineering 2 (2010): 1025-1034.

[2] C. Berger, B. Pyttel, T. Trossmann: Very high cycle fatigue tests with smooth and notched specimens and screws made of light metal alloys. International Journal of Fatigue 28 (2006): 1640-1646.

5.2 High cycle fatigue behaviour of laser beam welded Ti-6Al-4V butt joints subjected to postweld heat treatment

F. Fomin, V. Ventzke and N. Kashaev (HZG)
Contact: fedor.fomin@hzg.de

Laser beam welding (LBW) is a very promising joining technique for Ti-6Al-4V structural components aiming at cost and weight reduction since it provides the possibility of the high productivity, a single-step process and the benefit of potential weight savings compared with riveting. Despite generally higher static tensile strength [1], inferior fatigue properties of the laser beam welded titanium joints are commonly observed [2]. Since Ti-6Al-4V alloy is primarily used in fatigue-critical components, poor fatigue behaviour of the LBW Ti-6Al-4V joints is one of the main factors limiting their wide industrial application. The current study was undertaken in order to identify the main reasons for inferior fatigue properties of the LBW Ti-6Al-4V butt joints, quantitatively characterize the effects of surface quality, amount of welding defects and residual stresses on the fatigue behaviour, and provide suitable type of postweld heat treatment (PWHT) to increase the high cycle fatigue (HCF) performance.

The most frequently observed defects in laser weldments of titanium alloys are underfills and porosity [4]. These imperfections are particularly undesirable for structures subjected to cyclic loading because they lead to stress concentration and consequently premature crack formation. As shown in Figure 20(a) machining the weld underfills and reinforcements flush with the sheet surface can be considered as a relatively easy method to improve the fatigue performance of the LBW butt joints. Nevertheless, the S-N curve for the flush milled condition is located lower than that of the base material, as shown in Figure 20(a). The fatigue limit of the milled LBW butt joint is nearly 31 % lower than that of the base metal. This result implies the existence of internal defects deteriorating the fatigue strength of the joint.

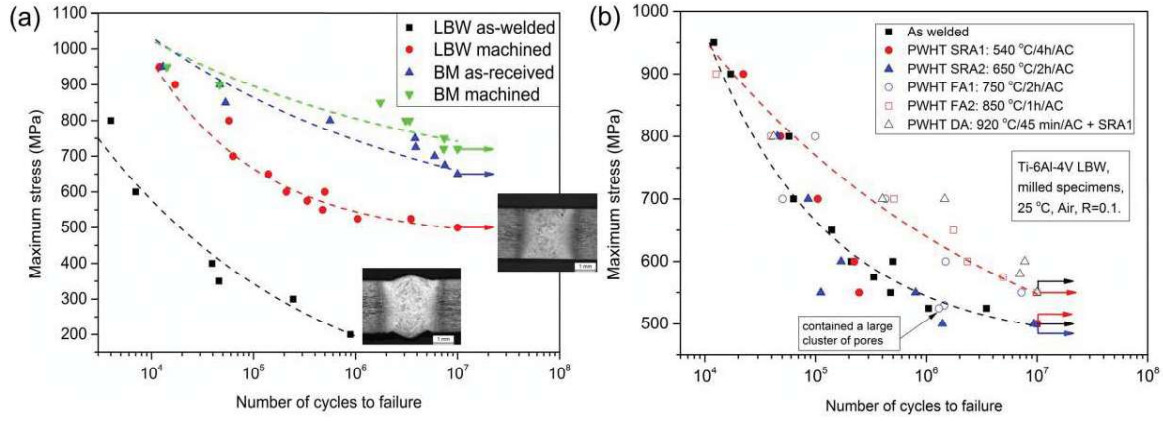

Figure 20: (a) Influence of machining on the fatigue behaviour of the base material and laser beam welded Ti-6Al-4V butt joints. (b) Effect of various types of postweld heat treatment on the fatigue properties of the milled laser beam welded Ti-6Al-4V butt joints.

Five types of PWHT in the temperature range of 540 – 920 °C were investigated. No significant effect on the fatigue performance was found for heat treatments with temperatures lower than 750 °C (Figure 20(b)). Since these temperatures are sufficient for achieving the full stress relief after welding, no significant influence of welding induced residual stresses on the HCF performance of the LBW Ti-6Al-4V butt joints was found in this work.

Annealing at temperatures higher than 800 °C increases the fatigue strength at 10^7 cycles by nearly 10 %, as shown in Figure 20(b).

Fractographical analysis of the fractured S-N specimens showed that almost 100 % of the failures started from pores with diameters of approximately 10 - 100 µm (Figure 21). These pores play the role of structural discontinuities and stress concentrators. The existence of such high stresses in the specimen leads to the initiation of the microcracks in very early periods of fatigue life.

Coarser lamellar microstructure (Figure 21(b)) displayed a more tortuous and deflected crack path than the finer-scale martensitic microstructure (Figure 21(a)) in the region adjacent to the pore, where the crack growth is sensitive to the microstructure. Increased crack path tortuosity leads to enhanced crack deflection and a resulting increase in the crack propagation resistance and the overall fatigue performance.

The area around the crack initiation site is slightly brighter than the region of stable crack growth (see Figure 21(c)). This white circle resembles a “fish eye” fracture, common for steels in the ultra-long-life regime [5]. So far, there is no published data on the “fish eye” type fracture for the LBW titanium alloys. Figure 21(d) shows the cross section of the specimen which endured 10^7 cycles and the crack nucleated from the subsurface pore.

The cracks found after high cycle fatigue testing bring us to the conclusion that major part of the fatigue life is spent for internal crack propagation within the “fish eye” and there is no fatigue limit at 10^7 cycles for the LBW Ti-6Al-4V joints. It implies that fracture mechanical approach should be used for fatigue life assessment of the LBW Ti-6Al-4V joints instead of safe life approach.

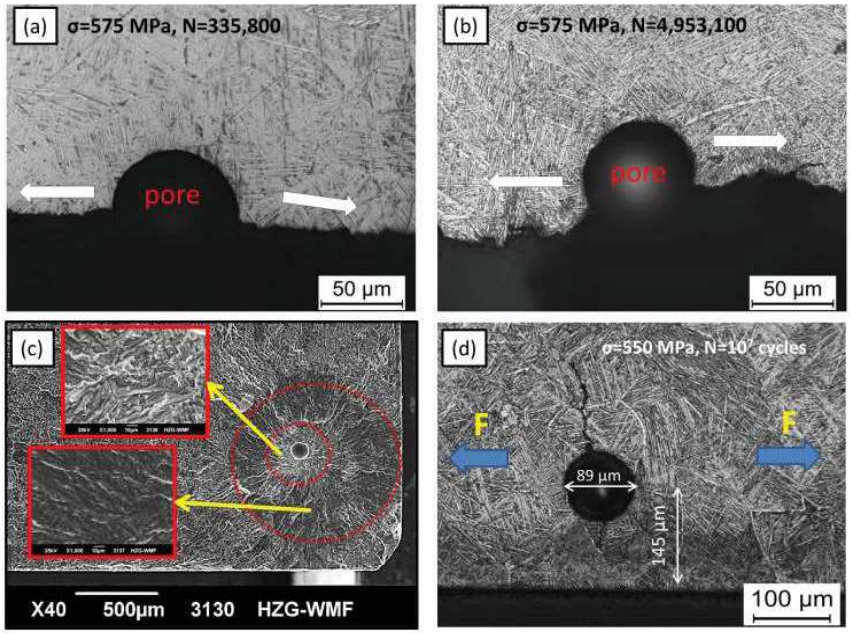

Figure 21: (a),(b) Comparison of the crack front profiles in the zone adjacent to the pore in the as-welded (a) and annealed at 850 °C for 1 h (b) conditions. (c) SEM images of fatigue fracture surface, distinct regions of the "fish eye" pattern are shown with higher magnification. (d) Transverse cross section of the specimen after 10^7 cycles with not propagating crack nucleated from subsurface porosity.

References

[1] N. Kashaev et al. (2016), *Opt. Las. Eng.*, 86, pp. 172-180.
[2] N. Kashaev et al. (2015), *Adv. Eng. Mater.*, 17(3), pp. 374-382.
[3] G. Lutjering (1998), *Mater. Sci. Eng. A*, A243, pp. 32-45.
[4] A.S.H. Kabir et al. (2012), *Metal. Mater. Trans. A*, 43(11), pp. 4171-4184.
[5] Murakami Y. (2002), Metal Fatigue, In: *Effects of small defects and nonmetallic inclusions*. 1st ed. Oxford, Elsevier.

5.3 Improvement of fatigue crack propagation behaviour through laser shock peening

N. Kashaev, V. Ventzke, M. Horstmann, S. Chupakhin, S. Riekehr and N. Huber (HZG)
Contact: nikolai.kashaev@hzg.de

Laser shock peening (LSP) has been successfully used for extending the fatigue life of critical components. LSP imparts residual stresses that are considerably deeper than those of traditional methods, such as sand blasting or shot peening. Several researchers investigated LSP for retarding the growth of long fatigue cracks and its effect on mechanical properties [1-3]. There are few studies that investigate the fatigue crack retardation mechanisms acting on a material with LSP-induced residual stresses. The goal of the current study is to understand the effects of LSP residual stresses on the fatigue crack propagation (FCP) behaviour of the commonly used aircraft aluminium alloy AA2024 with T351 heat treatment condition [4]. This alloy is generally used in aircraft applications requiring high strength to weight ratios as well as good fatigue resistance. The primary focus was to investigate the retardation effect of LSP-induced residual stresses on the FCP.

The LSP treatment was performed on C(T) specimens of aluminium alloy AA2024 with a thickness of 2.0 mm using a pulsed high energy Nd:YAG laser (Figure 22(a)). The obtained results indicate that LSP is an effective process for introducing high and deep compressive residual stresses without severe surface damages and deformations in the microstructure of thin AA2024 specimens. LSP is already an established process in aerospace industry for extending the fatigue life of critical thick-section components and the relevant laser and robot technology is commercially available. The results of this study can be similarly transferred to industrial LSP facilities designed for treatment of small-sized components as well as large scale structures.

Specimens with the LSP treatment reveal a significant retardation of the FCP rates (Figure 22(b)). Fatigue cracks suffered several crack closures in the region with compressive residual stresses. The presence of crack closure was confirmed through the presence of a frictional contact surface, thus leading to a smoothened surface topography. This effect was not observed in the BM, where shear fracture, fatigue striations, fatigue lines and fracture paths were clearly visible. Furthermore, the additional contribution of residual stress to the closure level was seen in the load vs. crack opening displacement curves. The presence of compressive residual stresses caused the more pronounced crack closure effect, which increased the level of opening load and therefore reduced the effective load range, $R_{F\,eff}$ (Figure 23(a)).

An original methodology on how to consider LSP-induced residual stresses on the FCP behaviour was proposed. It was shown, that the effective stress intensity factor range can be calculated based on the experimentally obtained load vs. crack opening displacement curves. By considering the effects of tensile and compressive residual stresses on the effective load range for the calculation of the stress intensity factor range, i.e., the so-called effective stress intensity factor range, ΔK_{eff}, the *da/dN* vs. ΔK_{eff} curves for the LSP treated specimens are close to the curve of the BM specimen

(Figure 23 2(b)). It is evident that the applied corrections for calculating ΔK_{eff} are reasonable and consider the effects of the tensile/compressive residual stresses induced by the LSP treatment.

Based on the obtained results and taking into account industrial LSP facilities the technology can be considered as a potential tool for the surface treatment of aluminium alloy airframe structures. Two possible application scenarios, where LSP can also be applied on thin structures, could be considered: design and repair. If the retardation effect of LSP-induced residual stresses can be predicted for a structural component, aircraft structures can be designed accounting for the LSP-induced residual stresses to improve the damage tolerance behaviour. The significant retardation effect of LSP on FCP behaviour can be used for repair of structural components, where small cracks are detected. Here, LSP treatment can be used to arrest cracks and decelerate the FCP.

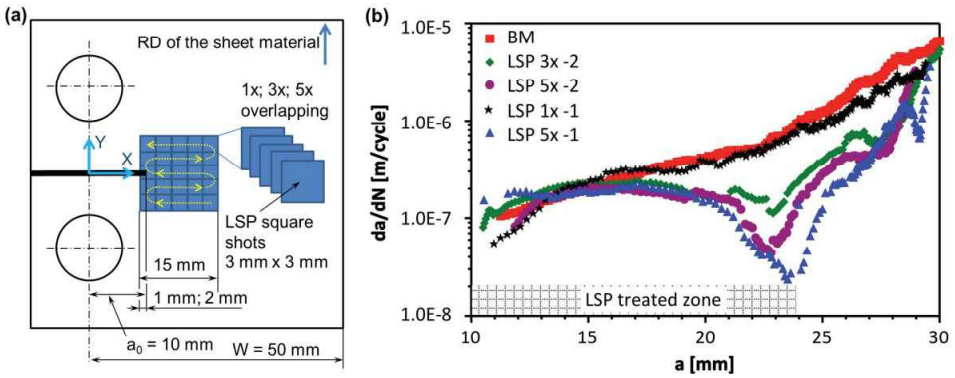

Figure 22: (a) Positioning of the LSP patterns on the C(T) specimen; and (b) FCP test results.

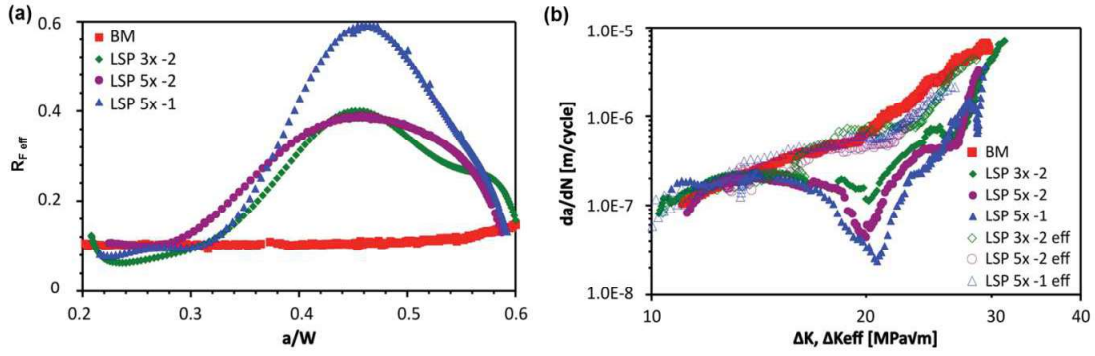

Figure 23: Correction of effective values under consideration of the LSP-induced residual stresses. (a) $R_{F\,eff}$ vs. *a/W,* and (b) *da/dN vs.* ΔK and ΔK_{eff}.

References

[1] O. Hatamleh et al. (2007), *Int. J. Fatigue*, 29(3), pp. 421–434.
[2] O. Hatamleh (2009), *Int. J. Fatigue*, 31(5), pp. 974–988.
[3] E. Hombergsmeier et al. (2014), *Adv. Mater. Res.*, 891-892, pp. 986-991.
[4] N. Kashaev et al. (2017), *Int. J. Fatigue*, 98, pp. 223-233.

5.4 Laser Shock Peening as Surface Technology to extend Fatigue Life in Metallic Airframe Structures

Domenico Furfari, Nikolaus Ohrloff (Airbus)
Elke Hombergsmeier, Ulrike C. Heckenberger, Vitus Holzinger (AGI)
Contact: domenico.furfari@airbus.com

The use of surface technologies inducing residual stresses can be employed in aeronautical industry as technologies to ensure salvage for identified hot spots in terms of fatigue and crack growth performance. Degradation processes, such as fatigue, limit service lives of aircraft structures. Technologies and methodologies that improve the resistance of structures to these degradation processes are of benefit to the aircraft industry in terms of extending the service life of the structure and thus reducing maintenance costs. An emerging technology is Laser Shock Peening, which can be used in lieu of conventional Shot Peening to introduce residual compressive stresses to a metallic structure. This engineering field can be identified as Residual Stresses Engineering aiming at improving the economic and ecological impact of an aging fleet as well as of future aircraft structures by controlling the residual stresses.

Here an overview is provided how this technology can enhance fatigue and crack growth for different metallic materials commonly used in aircraft structures: ranging from Al alloys (2024-T351, 7010-T7451) to Precipitation Hardened Stainless Steel X3CrNiMoAl13-8-2. The depth of the compressive residual stresses is controlled by the laser peening parameters to obtain the “desirable” residual stress profile with the aim to inhibit fatigue crack initiation and crack propagation as function of the thickness.

Through thickness compressive residual stresses can be obtained treating the two opposite surfaces of Al sheets (i.e. Al2024 and Al7050) up to a thickness of 6mm, controlling the extension of the tensile residual stresses (auto balanced stresses) outside the processes areas to avoid undesirable increase of stresses at other critical locations (see Figure 24). Both Al2024-T351 clad and unclad material (2mm thick) where laser peened and fatigue tested under constant amplitude loading showing the capability to slow down through thickness crack growth when the crack front crossed the compressive residual stress field. It was possible to obtain through thickness compressive stresses firing the laser directly onto the Al clad layer at the surface of the specimens without prior clad layer removal. The residual stress field induced by the laser shock peening process was characterized with hole drilling technique as well as non-destructive testing such as X-Ray Diffraction and Synchrotron diffraction. Tests on CCT (Centre Crack Tension) specimens made of Al2024-T351 have shown a dramatic reduction of the crack propagation rates (an order of magnitude compared with reference material) at a stress intensity factor ranging from 30MPam$^{1/2}$ to 50MPam$^{1/2}$.

Most works on LSP have utilized a Neodym-YAG laser with its fundamental wavelength of 1064 nanometers in the near infrared or Neodym glass lasers (fundamental wavelength at 1054 nanometers) in combination with an applied absorption/insulation layer (usually a thin aluminum foil). This additional Al layer, which vaporizes during the laser pulse forming the plasma pressure and the consequent pressure shock wave travelling into the material, is also used to prevent the surface from melting or being damaged during peening (as a sort of sacrificing layer). When the laser process was used without

the prior application of the Al ablative layer (i.e. laser peening onto bare material) the status of the surface was studied and it was found that the thermally affected layer caused by the high temperature during the peening (although only for a duration of 20 nanoseconds) left the first 5-10µm of material without compressive residual stress or slightly in tension. A laser peening coverage above 300% brought back the compressive residual stresses at the near surface of the treated material. For high production rates or to make the application of laser shock peening in some specific aircraft components economical more attractive it could be a valid solution to carry out the treatment without ablative coating which is normally a manual operation slowing down the manufacturing rate significantly.

Surface treatments such as Chromic Acid Anodizing (CAA) and Tartaric Sulfuric Anodizing (TSA) are typical surface protections applied in Al structures to prevent from corrosion damages. Structural coupons made of Al7050-T7451 and Al7010-T7451 of 30 mm thickness containing a stress concentration factor of 2 and the surface treatments above described were fatigue tested under constant amplitude loading with stress ratios of: R=-3, R=-1.75, R=-1, R=-0.3 and R=0.1. Deep compressive residual stress induced on the surface by laser shock peening (minimum 3mm depth) demonstrated to be able to delay the fatigue crack initiation and the crack propagation in all ranges of R ratios tested providing for all conditions a significant fatigue life extension compared to conventional shot peening and ultra-sonic peening. The fatigue behavior was also studied in presence of the anodizing layer (see Figure 25). The capability of inducing deep residual stresses, firing laser shock peening directly onto the surface coating without prior removal, is an attractive alternative to the standard operation. The test campaign was completed with Variable Amplitude Loading fatigue tests demonstrating the capability of laser shock peening to delay the crack initiation and propagation compared to non-treated structural coupons.

Precipitation Hardened Stainless Steel X3CrNiMoAl13-8-2 has been selected, as typical high strength material commonly used in aeronautic structures, to investigate the fatigue and crack growth behavior after inducing compressive residual stress at the near surface by means of laser shock peening (see Figure 26). Residual stress measurements on round bar coupon of 35mm diameter using hole drilling and neutron diffraction techniques demonstrated the capability to introduce high compressive residual stresses at the near surface (-0.8YST of the material) with depth into the material of minimum 2mm. The effect of surface layer removal by fine machining (i.e. roughness of 0.8µm) after laser peening without ablative layer has been investigated. The effect on fatigue of laser peening without ablative coating and fine surface machining as well as with ablative layer without surface machining have been investigated to assess the fatigue behavior in unnotched flat coupons as well as round bar coupons having a stress concentration factor of 2 subjected to four point bending loading. The surface condition after laser peening with surface protection (ablative layer) in terms of roughness profile has been studied and will be reported. The crack growth behavior in deep residual stress field was part of the investigation and the experimental results are shown in Figure 26 as well. The specimens used for this type of test were round bar coupons with a stress concentration factor of 2 subjected to four point bending fatigue loading at variable amplitude loading condition. The initiation site at the stress concentration area was addressed by an EDM notch of 2.54mm x 1.27mm prior to fatigue pre-cracking. Potential

drop and optical techniques were used to monitor the crack growth as well as fracture surface investigations by SEM after the fatigue crack propagation test.

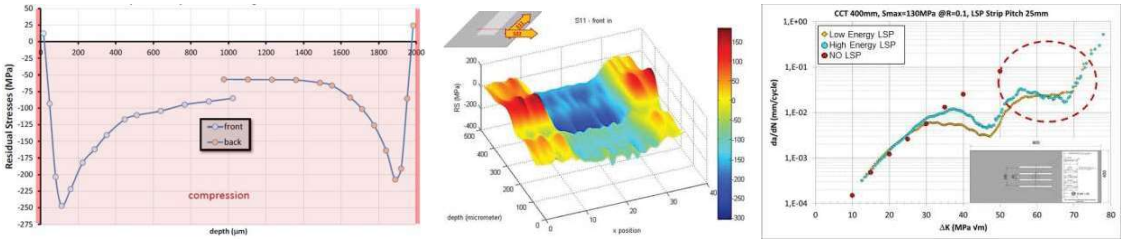

Figure 24: Through thickness compressive residual stress of A2024 clad material induced by Laser Shock Peening and crack growth test (left, hole drilling; center, synchrotron x-ray diffraction method, right crack growth test results)

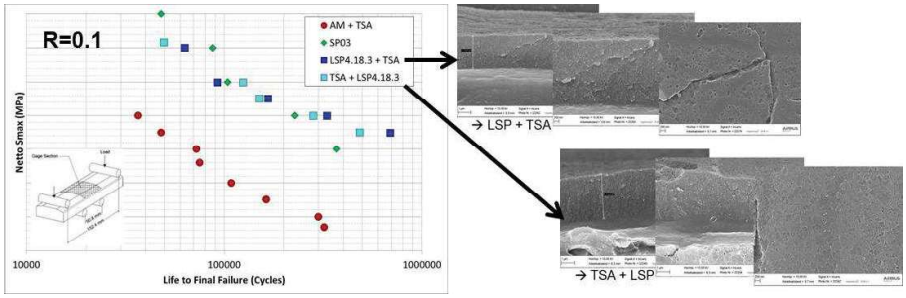

Figure 25: Fatigue test results on AA7010 material shown dramatic improvement in fatigue strength after Laser Shock Peening induced directly on anodized layer (Tartaric Sulfuric Anodizing), without prior removal

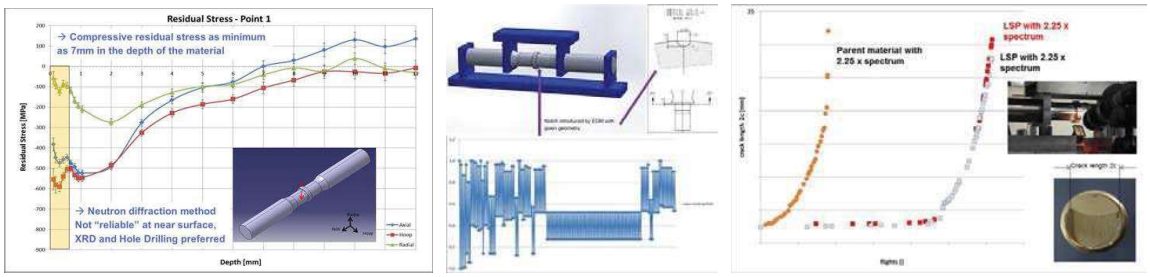

Figure 26: Compressive residual stress on X3CrNiMoAl13-8-2 up to 9mm depth (left); crack growth from rogue flaw to critical crack length have shown dramatic delay in crack growth compared to No LSP solution

References

[1] D. Furfari, N. Ohrloff, E. Hombergsmeier, U. C. Heckenberger, V. Holzinger, "Laser Shock Peening as Surface Technology to extend Fatigue Life in Metallic Airframe Structures", 5th International Conference on Laser Peening and Related Phenomena, Cincinnati, Ohio, USA, 11-15 May 2015.

[2] D. Furfari, N. Ohrloff, E. Hombergsmeier, U. C. Heckenberger, V. Holzinger, "Enhanced Fatigue and Damage Tolerance of Aircraft Components by Introduction of Residual Stresses – A Comparison of Different Processes", presented at 33rd ICAF Conference, Jerusalem, Israel, 3-7 June 2013.

5.5 3D-Printing-Technology *born-to-fly* by GROB Aircraft AG

Bernd Zapf (GROB)
Contact: B.Zapf@grob-aircraft.com

In the last years, the Industrial 3D printing / Additive Manufacturing (AM) of high-tech aerospace components became more and more attractive for series production. Engine and turbine parts as well as cabin interior components are typical applications for industrial 3D printing. Functional components with complex geometries and defined aerodynamic properties can be manufactured quickly and cost-effectively. Material and weight savings reduce fuel consumption and CO_2 emissions. Manufacturer-specific adaptations and small production runs are further arguments in favor of Additive Manufacturing technology. This is why leading aerospace companies have integrated AM into their planning of future production strategies.

The manufacturing process used at GROB Aircraft AG is the Laser Sinter (LS) process executed from Materialize. Laser Sintering, also known as selective Laser Sintering (SLS), is among the most versatile and frequently used 3D printing technologies.

The standard material for additive manufactured parts by Grob Aircraft is PA 2241 FR. It is a flame retardant polyamide 12 for processing in laser sintering systems. The condition before melting with laser is powder. It contains a halogen-based flame retardant. Mainly due to its recyclability, the material is economical, enabling low-cost part production. The main field of application of this material is for aviation interior or exterior, e.g. air ducts and air outlet valves.

The mechanical properties are dependent on building direction and differ in “dry” and “conditioned” data:

- “dry” refers to data that is obtained from a sample of material with equivalent moisture content as when it was molded (typically <0.2%) as specified in EN ISO 527.
- “conditioned” on the other hand, refers to data obtained from a sample of material that has absorbed some environmental moisture at 50% relative humidity prior to testing as specified in EN ISO 527.

All material properties are based, on tests with standardized test methods.
Without any coating protection the material is usable up to 84° Celsius (HDT/A) (Heat Deflection Temperature) and 154° Celsius (HDT/B). The values are based on standardized tests for viscoelastic plastics acc. to EN ISO 75. The test specimen is loaded in three-point bending in the edgewise direction. The outer fiber stress used for testing is either 0.455 (HDT/B) MPa or 1.82 (HDT/A) MPa, and the temperature is increased at 2 °C/min until the specimen deflects 0.25 mm. The value for HDT/A correlates with the temperature where the strength of the material drops in very fast. So for future designs the limit operation temperature is the value of HDT/A, unless otherwise specified.

The material PA 2241 FR, had passed the Vertical Bunsen Burner Test acc. to CS25/JAR25/FAR25 §25.853 (a) App. F Part I. The smoke generation was tested by ABD 0031 (Issue: F), method: AITM 2.0007. In addition, the toxic gas generation was tested by ABD 0031 (Issue: F), method: AITM 3.0005. All tests were passed and meet the requirements.

In a post-production process, the manufacturer can optionally smooth the surface with vibratory finishing and/or protect the part with color infiltration against discoloration by UV-radiation. The infiltration is available in different colors. For applications on outer surface of the aircraft, the parts can be coated with special plastic filler and a finishing paint to protect the surface against environmental influence. At the present, there is no experience about the correlation of post-production processes with the mechanical properties.

The growth of different microorganism like harmful mold was analyzed acc. to EN ISO 846. No visual growth of microorganisms could be microscopically detected.

The Certification of the AM Parts is according to the Certification Memorandum Additive Manufacturing EASA CM No.: CM–S-008 Issue 01 issued 04 April 2017

Example for additive manufactured parts is the Canopy Camera Mount System:

- The camera mount canopy is mounted at the upper rear of the canopy, holding a small camera, see Figure 27 below.
- Infiltrated with black color (RAL 9005) for UV-resistance and perspiration-proofness
- Integrated printed part no. and company logo.

Figure 27: Camera Mount Canopy (cam 1) and mounting position

6 Fatigue and Fracture of Composites

6.1 A physically based damage model for composite structures including three-dimensional stress states

H. Madhusoodanan, E. Jansen, R. Rolfes (ISD)
Contact: h.madhusoodanan@isd.uni-hannover.de

In the last decades there has been an intensive research activity in the field of modeling the fatigue behavior of fibre-reinforced plastic (FRPs). The models investigated can be classified into three groups – fatigue life concepts, phenomenological models and progressive damage models. A recently developed layer-based fatigue damage model (FDM) by Krüger [1-2], addresses several shortcoming of the existing fatigue models and at the same time enables the fatigue analysis of larger structures. Due to the energy-based methodology and in combination with the fracture-mode dependent theory of Puck [3], the model is considered to be physically based. The two-dimensional approach with efficient standard shell elements as well as a block-wise loading approach makes the fatigue assessment of large structures (e.g. rotor blades of wind energy turbines) possible.

The original, two-dimensional (2D) FDM is based on classical laminate theory (CLT) and as a result five degradation factors are required for definition of both strength and stiffness at different layers. These degradation factors also take into account the material orientation (longitudinal or transverse to fibre direction) as well as the type of loading (tension, compression or shear). The FDM has two main parts, the discontinuous degradation analysis, which takes into account the degradation due to the quasi-static loading, and the continuous degradation analysis resulting in the degradation due to repetitive loading. The FDM has been implemented in the commercial finite element code ABAQUS through a user written material subroutine ‘UMAT’ and used together with the standard shell elements. For the validation of the FDM, the resultant strength degradation parameters were verified with the results from OptiDAT-Data bank [4].

In complex situations such as delaminations or multi-dimensional loading conditions like bending or torsion, the use of CLT is not appropriate. In order to analyze such complex load cases, the existing FDM has to be modified to take into account the stresses and degradation in all relevant directions. In the context of DFG, Special Priority Program, SPP 1466 [5], which deals with the experimental and numerical investigations on metals and composites in the very high cycle fatigue (VHCF) regime, the existing 2D FDM has been extended to the three-dimensional (3D) framework. For this extension, appropriate modifications are made to the constitutive relations and also the Puck [3] failure criteria were modified to take into account the 3D stress state. Assuming transverse isotropy, the quasi-static stress-strain relations as well as the essential fatigue strain evolution curves and their method of degradation remain unchanged in the 3D extension approach. While in the 2D approach layer-based shell elements are used, the extended version comprises the use of a finite element model based on solid elements, which makes the applicability in a 3D framework possible.

Recently, experimental investigations for the VHCF behavior of GFRP specimens have been carried out using a four-point bending setup [6]. In these experiments, the reduction in bending stiffness due to fatigue damage is analyzed. This representative case illustrates the capabilities of FDM and its 3D extension. For the purpose of fatigue simulation, two models are created, a shell based model for the 2D FDM and a solid based element for 3D FDM as shown in Figure 28b and Figure 28c, respectively. The element type chosen for the 2D FDM are the reduced integrated shell elements (S4R), whereas for the 3D FDM fully integrated solid brick elements (C3D8) are chosen. Figure 29a and Figure 29b compares the variation of the displacement amplitude (due to bending) obtained for different load levels (*LL1, LL2 and LL3)* for both 2D and 3D FDM to that of the displacements determined from the experiments. It can be seen in Figure 29 that the results of both 2D and 3D FDM are in good agreement with the experimental results.

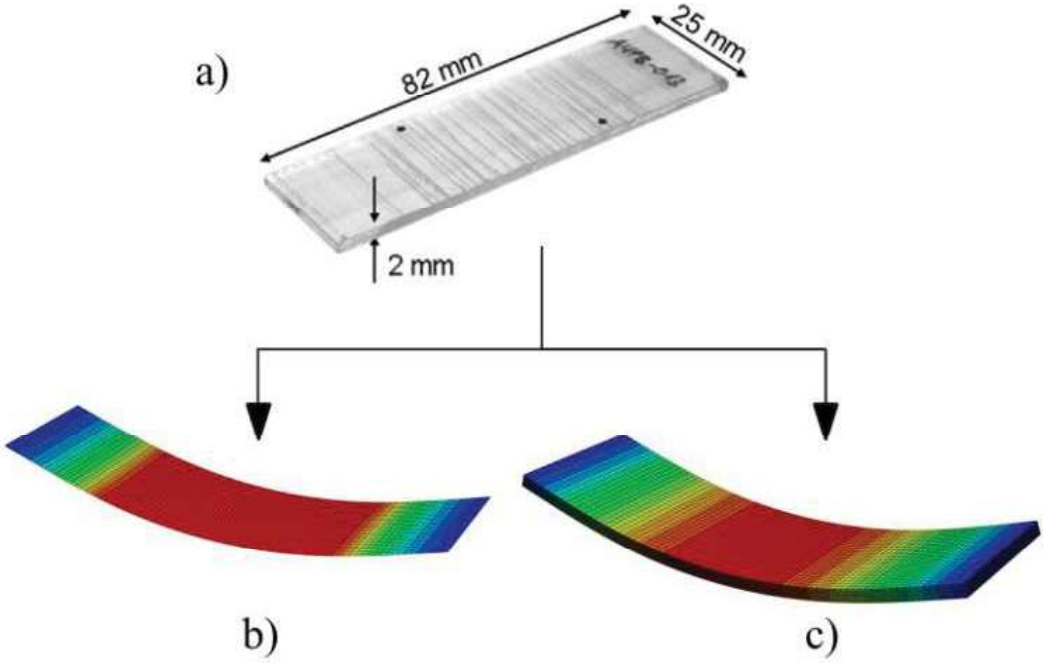

Figure 28: a) GFRP specimen used in the four-point bending test in VHCF regime [6]; b) Finite elment modelling of the specimen - b) using shell elements and c) using solid elements.

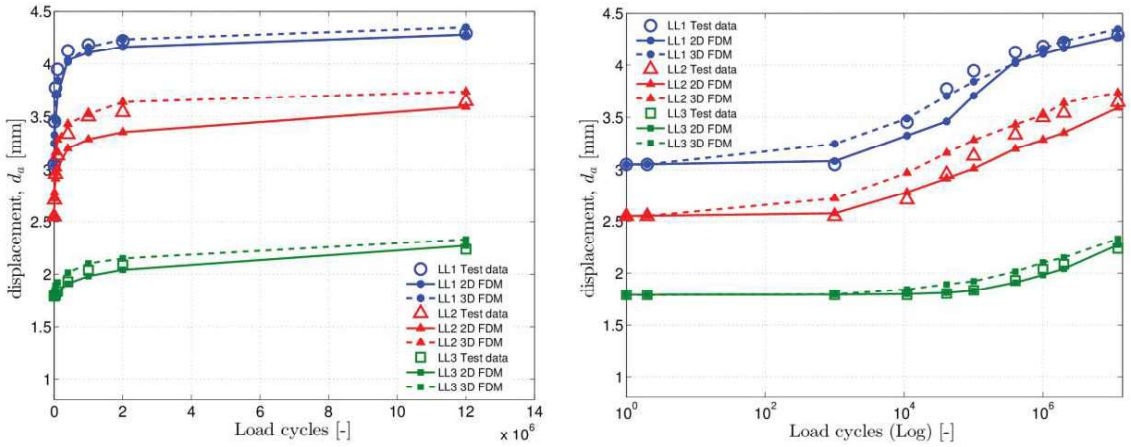

Figure 29: a) Comparison of 2D and 3D FDM with respect to the experimental results for load levels LL1 to LL3 (expressed in normal scale) b) Comparison of 2D and 3D FDM with respect to the experimental results for load levels LL1 to LL3 (expressed in logarithmic scale).

References

[1] H. Krüger: 'Ein physikalisch basiertes Ermüdungsschädigungsmodell zur Degradationsberechnung von Faser-Kunststoff-Verbunden', PhD thesis, Raimund Rolfes, editor. Institute of Structural Analysis, University of Hanover, Germany, 2012. (ISSN 1862-4650)

[2] Heiko Krüger, Raimund Rolfes: 'A physically based fatigue damage model for fibre-reinforced plastics under plane loading.', International Journal of Fatigue, 2015, 70, 241-251.

[3] A. Puck: 'Festigkeitsanalyse von Faser-Matrix-Laminaten – Modelle für die Praxis.', Munich, Germany, Carl Hanser Verlag, 1996. (ISBN 3-446-18194-6)

[4] OptiDAT: 'Optimat Blades Database, database reference document, R. Nijssen. OB_TC_R018 rev. 004, Ver. 1.9.6', WMC, Netherlands, June 2006. https://www.wmc.eu/optimatblades_optidat.php.

[5] SPP 1466: 'Schwerpunktprogramm „Life ∞ – Unendliche Lebensdauer für zyklisch beanspruchte Hochleistungswerkstoffe" (SPP 1466) Zweite Phase: 2013-2016.', 2016, http://www.dfg.de/foerderung/info_wissenschaft/2012/info_wissenschaft_12_47/index.html

[6] T.J. Adam, P. Horst: 'Experimental investigation of the very high cycle fatigue of GFRP [90/0]s cross-ply specimens subjected to high-frequency four-point bending.', Composite Science and Technology, 2014, 101, 62-70.

6.2 Improvement of the cyclic loading resistance of highly loaded CFRP components by resin modifications

J. Krummenacker, A. Klingler, J. Hausmann, B. Wetzel (IVW)
Contact: joachim.hausmann@ivw.uni-kl.de

The Institute for Composite Materials developed an application oriented evaluation methodology and analyzed various resin modifications in order to augment the lifetime of carbon fiber reinforced epoxy (CFRP) laminates. The project with several partners along the process chain uses the example of flywheel energy storage applications. However, the results are transferable to any other highly loaded CFRP component.

A finite element based stress analysis of the flywheel component revealed that the laminate is mostly exposed to tensile stresses parallel to the fiber direction and thus fiber breakage shows to be the most critical fracture mode under quasi-static loading conditions. Furthermore, due to the special lay-up configuration of the flywheel, the laminate is also subjected to high interfiber, hence matrix stresses. As the resistance to interfiber fracture decreases faster under cyclic loading than the resistance to fiber fracture, the laminate will first undergo interlaminar failure, which can lead to stress concentrations and hence accelerate the final failure. Therefore, the presented research is based on the hypothesis, that the fatigue resistance of a CFRP is dominated by its matrix behavior, more specifically the ultimate strain.

To increase the ultimate strain of the matrix system various approaches were pursued, e.g. making use of additional micromechanical mechanisms introduced into the brittle epoxy system by a particulate or chemical modification. The flywheel component manufacturing is done by filament winding and requires a low resin viscosity for a proper fiber impregnation. Therefore, a crucial parameter for the workability was also not to alter the viscosity of the resin systems by varying its composition.

To analyze and verify the workability, the (fracture) mechanical, viscoelastic and thermal properties of the modified resin systems, with respect to an anhydride cured cycloaliphatic reference epoxy system (EP1), were systematically examined and characterized (Figure 30). During this extensive modifier screening three systems were identified as the most promising ones, meaning an elevated ultimate strain and still meeting the other requirements. The first system, a core-shell rubber (CSR) toughened aromatic epoxy system (EP2), showed a tremendously increased ultimate strain due to crack pinning effects and plastic void growth of the matrix material. However, the glass transition temperature was reduced. A second approach was the synergistic reduction of the crosslink density into the reference system (EP1-mod) and the introduction of CSR which doubled the ultimate strain with respect to the reference system. Finally, functionalized carbon nanotubes (CNT) were mechanically dispersed via a three-roll calendar in the reference system, which were found to be beneficial for improving the mechanical properties as well as the fracture toughness.

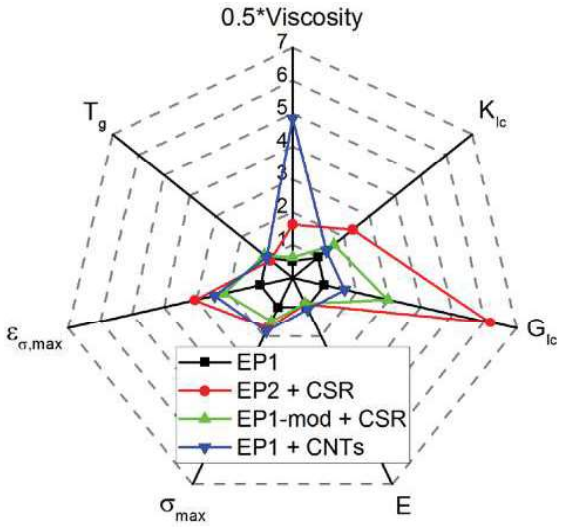

Figure 30: Mechanical and thermal properties of various resin systems relative to reference.

In addition to the survey of the matrix modifications, the decisive stress and strain distribution in the fly-wheel was computed using finite element analysis. Subsequently, a cyclic test method was searched for that allowed to reproduce the stress state in the fly-wheel and at the same time can be performed with wound specimens. These requirements lead to the adaption of the split-disc method for cyclic loading. The test set-up consists of two discs that are pulled apart (Figure 31, left). For the monitoring of possible stiffness degradation an additional displacement sensor was used.

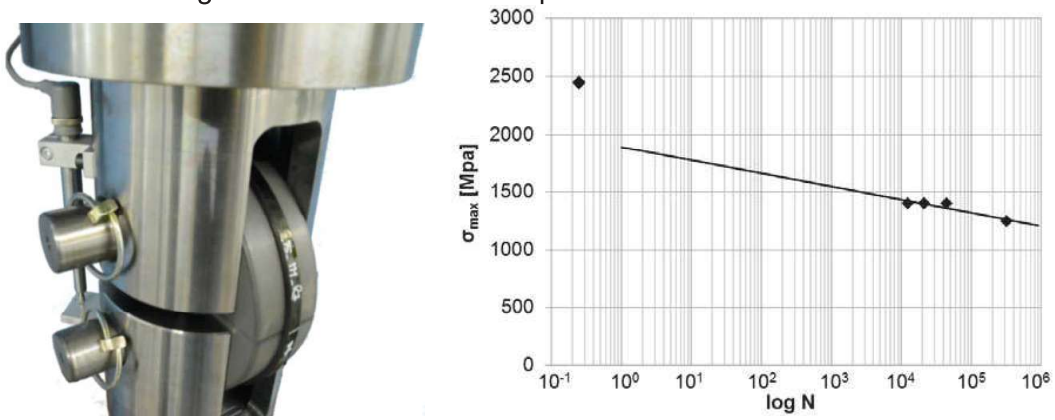

Figure 31: left: Test set-up of cyclic split disc-method; right: Lifetime of filament wound rings of the reference material.

Laminates made of the reference matrix were tested at different stress levels leading to a lifetime curve (Figure 31, right). The three modified matrix systems are currently being tested with the objective to compare the resulting lifetime curves. These - for the example of a flywheel – developed methods and results can be adapted to various other applications.

Acknowledgement
The project „Cyclic loading resistant resins for energy storage applications” is funded by the AiF within the ZIM program.

7 Fatigue and Fracture of Engine Materials

7.1 Influence of systematic pre-ageing on crack initiation and propagation in a coated superalloy during low cycle fatigue at 950°C

J. Wischek, A. Subramaniam, L. Chernova, M. Bartsch (DLR)
Contact: Marion.Bartsch@dlr.de

Nickel based superalloys are well known for their good mechanical properties at high temperatures. Therefore they are used for applications in stationary gas turbines and jet engines, such as for turbine blades, which are the thermally and mechanically most stressed components. To protect the superalloy material against oxidation during long term use, turbine blades are usually coated with metallic layers, which form protective oxide layers. During service, the exposure to high temperatures causes changes in the microstructure of the coated system, such as oxidation, grain growth, and phase reactions, which evolve simultaneously to fatigue damage and influence the damage behaviour under fatigue loading. Investigating the damage evolution in laboratory under real time conditions would be extremely time taking, considering a typical service life time of a turbine blade of about 5,000 to 20,000 hours. Therefore, one strategy in accelerating laboratory testing is to apply time dependent damages by pre ageing of multiple specimens in a furnace and further apply realistic number of cycles but with high frequency. Since fatigue and time dependent processes typically interact with each other, separation of ageing and fatigue may give misleading results for lifetime assessment in service. In this work interaction between ageing and fatigue mechanisms has been systematically investigated on superalloy specimens with an oxidation protection coating by applying on differently pre-aged specimens an identical isothermal LCF load sequence.
Low cycle fatigue (LCF) experiments have been performed at 950°C with R = -1 under strain control on specimens made from cast nickel-based superalloy IN 100 coated with a NiCoCrAlY oxidation protection layer. Specimens were tested after processing and systematic pre-ageing, respectively. The LCF tests were interrupted after defined number of cycles, and the specimens were investigated by microscopic and microanalytic methods for characterizing the effect of systematic pre-ageing on crack initiation and propagation. The microstructural evolution due to ageing only has been systematically investigated on separate specimens in order to achieve information on interaction between fatigue and ageing.

Main effects of pre ageing on the microstructure of the coated system were (1) a thermally grown oxide (TGO) layer formed on the coating surface, (2) roughening of the surface occurs, which is also called rumpling. Such rumpling is well known, a phenomenon driven by the lengthening of the TGO, which is intruding into the underlying metal at local instabilities [1], (3) grain growth occurred in the metallic coating, (4) at the interface between substrate and coating a diffusion zone with intermetallic phases evolved, and (5) small edged chromium carbide precipitates evolved in the substrate near the diffusion zone.

Main observations with respect to damage evolution during the LCF sequence were (1) fatigue cracks were initiated at the oxidized surface, predominantly at rumpling instabili-

ties of the TGO and number of cracks initiated was increasing with ageing time, (2) crack propagation was decelerated with pre ageing time by enhanced crack deviation and branching in the metallic coating, at the diffusion zone, and in the substrate near the diffusion zone. Examples of fatigue cracks in differently pre aged specimens are given in Figure 32.

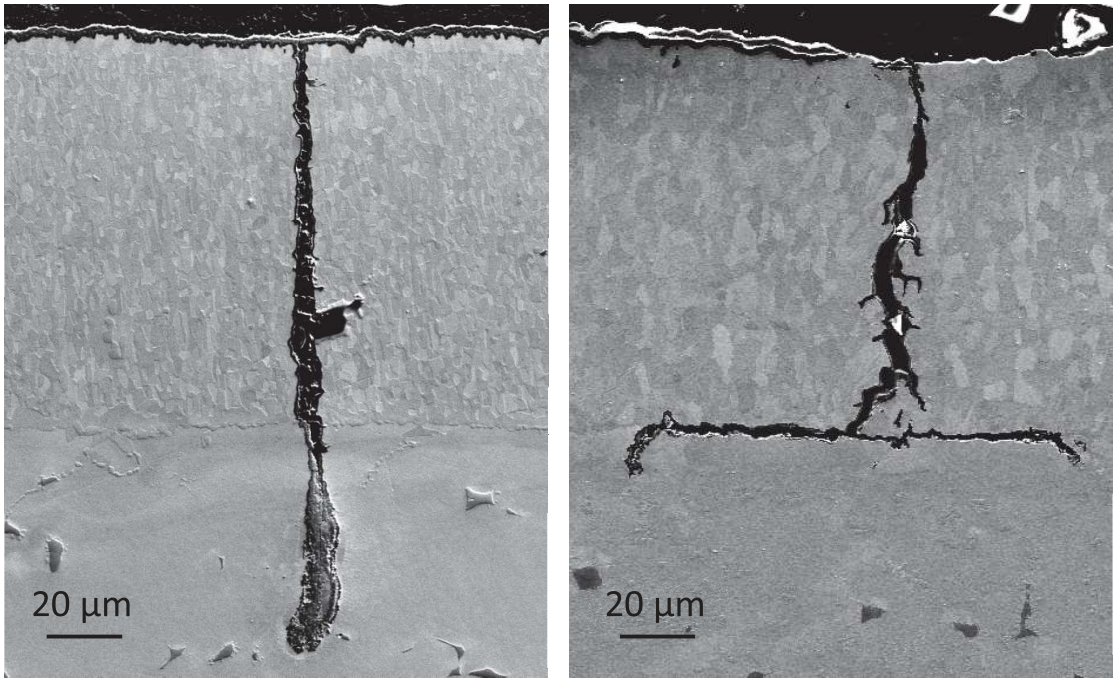

Figure 32: Examples of crack propagation during 20,120 LCF cycles in a specimen pre aged for 25h (a) and for 875h (b)

The obtained results reveal complex interaction of mechanisms due to ageing and LCF loading. With respect to strategies of accelerated testing by applying ageing time and fatigue separately, the interaction between time and number of cycle dependent mechanisms has to be explored before extrapolating laboratory results to lifetime assessments under service conditions.

For the actual example however, it seems that controlled pre ageing has a potential to elongate service life of components with a metallic coating, since not the number of cracks in the coating but the extension of fatigue cracks into the substrate is lifetime limiting.

Reference

[1] J. Shi, A.M. Karlsson, B. Baufeld, M. Bartsch: Evolution of surface morphology of thermo-mechanically cycled NiCoCrAlY bond coats, Mat. Sci. & Eng. A434 (2006) 39-25.

8 Non-Destructive Testing

8.1 NDT Procedure Development for Bombardier Global 5000/6000 Series

Christoph Prüfer (IABG)
Contact: hilfer@iabg.de

IABG was performing NDT (Non-Destructive Testing) inspections along the DURABILITY AND DAMAGE TOLERANCE TEST (DADTT) for the type certification of Bombardiers CSeries (BD500) CS100 / CS300 aircraft family started on schedule in August 2014.

Based on this collaboration IABG was asked to support Bombardier Aerospace on the development of NDT procedures for Bombardiers Global 5000/6000 Series.

Project Breakdown:

1. Preparation Phase
    a. DMU (Digital Mock-Up) Analysis
2. CRS (Calibration Reference Standard)
    a. CRS design
    b. CRS manufacturing
3. Procedure Development
    a. drafting of NDT procedure
    b. validation on CRS
    c. RT validation on serial aircrafts
    d. final development of NDT procedure
4. Procedure Validation
    a. validation on serial aircrafts
    b. final validation by customer

NDT procedures are needed during maintenance checks based on MSG-3-derived maintenance programs. The scope of the project was focused on metallic Principal Structural Elements (PSEs). Eddy Current (ET, Ultrasound (UT) and Radiography (RT) were the chosen NDT methods to detect surface and subsurface cracks reliably.

Calibration Reference Standards (Figure 33) are needed to calibrate the inspection system on defined notches to assure the detection of sub-surface cracks on aircraft structure. The design and manufacturing of CRSs were also included in this project. Electrical Discharge Machining (EDM) was used to minimize the thickness of the artificial crack to 0,010 mm.

In total 22 NDT procedures were developed and 13 CRS were designed and manufactured.

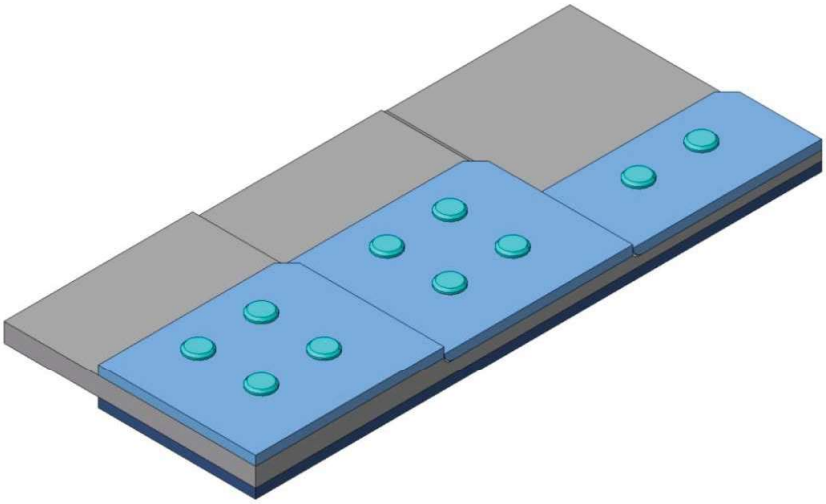

Figure 33: Example of a Calibration Reference Standard